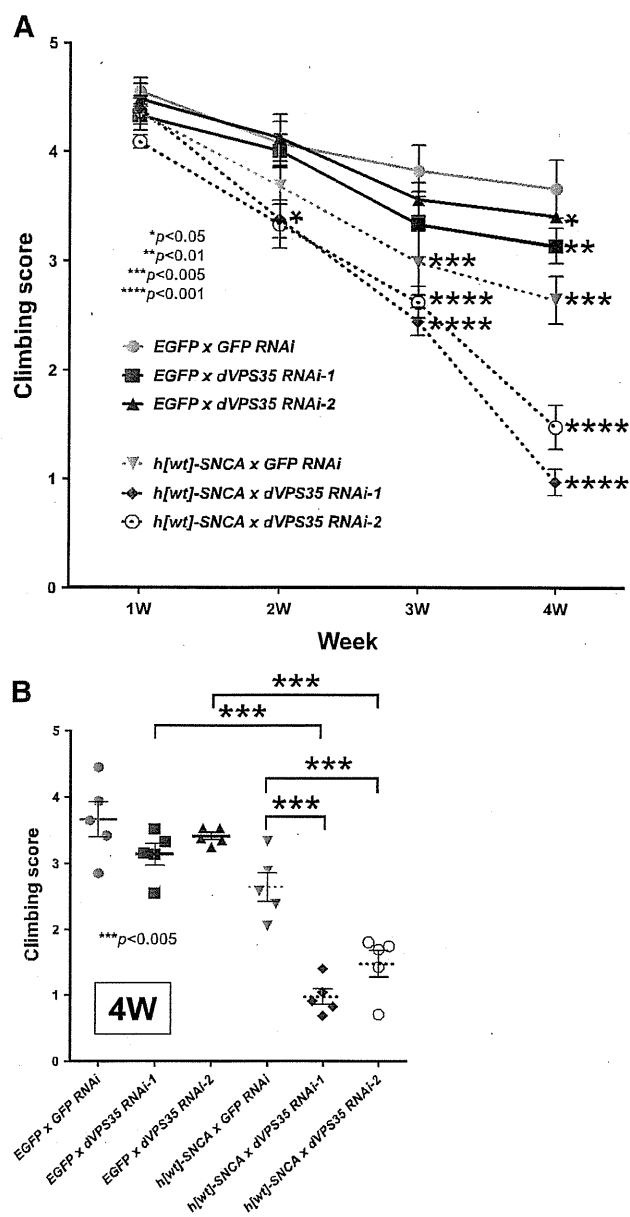


**Fig. 4.** Silencing of *dVPS35* induces mild eye disorganization in human  $\alpha$ SYN transgenic *Drosophila*. (A) Eye-specific expression of *h[wt]-SNCA* with *dVPS35* RNAi resulted in compound eye disorganization. The eye phenotype was normal in 1-week-old transgenic flies over-expressing *h[wt]-SNCA* with *GFP* RNAi. By contrast, when *dVPS35* was silenced, the *h[wt]-SNCA*-Tg flies showed a slight shrinkage of each ommatidium with disarrayed bristles compared to the control flies expressing both *h[wt]-SNCA* and *GFP* RNAi or both *EGFP* and *dVPS35* RNAi. The white square indicates the magnified area. Scale bar: 100  $\mu$ m. (B) For the quantification of intact interommatidial bristle numbers, the number of visible bristles was counted and divided by the total number of ommatidium. Note that the silencing of *dVPS35* in *SNCA* transgenic flies significantly decreased the numbers of bristles compared to other fly lines. The pooled data were statistically analyzed by a one-way ANOVA followed by a Bonferroni multiple comparison test. \* $p < 0.001$  ( $n \geq 10$ ).

highly conserved PRLYL motif at the N-terminus destabilizes VPS26 and disrupts cargo sorting in the prevacuolar endosome and retrieval of the retromer to the TGN, indicating that this mutation converts VPS35 to a dominant-negative protein in *Saccharomyces cerevisiae* (Zhao et al., 2007). Similarly, in a rat insulinoma cell line, the exogenous expression of the human VPS35 R107W mutant (the functional equivalent of the R98 residue in yeast) has an altered intracellular membrane distribution that perturbs a number of post-Golgi trafficking functions (Zhao et al., 2007). Moreover, a recent study has shown that the expression of

D620N VPS35 induces the marked degeneration of dopaminergic neurons both in primary neuron culture and in a rat model (Tsika et al., 2014). These findings suggest that mutant VPS35 may have an influence on retromer function via a potentially toxic gain-of-function with a dominant negative effect. This notion is supported by a recent observation demonstrating that the PD-linked VPS35 D620N mutation disrupts the cargo-sorting function of the retromer, causing an abnormal trafficking of CTSD (Follett et al., 2014). We also produced the over-expression of the PD-linked mutant VPS35 (D620N and P316S) in



**Fig. 5.** RNAi-mediated silencing of *dVPS35* deteriorates locomotor function in human  $\alpha$ SYN transgenic *Drosophila*. (A) Knockdown of *dVPS35* induced an age-dependent decline in climbing performance in flies expressing the human  $\alpha$ SYN in the nervous system. Five trials were performed in each group at 20 s intervals and the climbing index was calculated. Results are presented as the means  $\pm$  standard errors of the scores obtained in 5–10 independent experiments. All climbing assay experiments were conducted at 25 °C. The *Elav-GAL4* driver was used for the experiment. (B) In order to make it easier to compare each climbing performance in different fly lines, the climbing scores of 4-week-old flies are also presented as a categorized scatter plot with mean segments. Pooled data from at least 5 experiments were statistically analyzed. \* $p < 0.05$ , \*\* $p < 0.01$ , \*\*\* $p < 0.005$ , and \*\*\*\* $p < 0.001$  (two-way ANOVA with the Bonferroni multiple comparison test;  $n \geq 5$ ).

HEK293 cells to determine its distinct influence on retromer function. Unexpectedly, not only the exogenously expressed mutants, but also the wt VPS35 equally resulted in the aberrant trafficking of CI-MPR together with the impaired maturation of CTSD. This finding is apparently contradictory to a report by Follett et al., which demonstrated that exogenous expression of the mutant D620N, but not the wt VPS35, abnormally traffics CI-MPR in HEK293 cells, resulting in the incorrect processing of CTSD. Although the reasons for these discrepancies are not clear, a possible explanation is the difference in the protein

expression level in each experiment. The retromer requires an apparent equimolar stoichiometry of the subunit to exert its normal function (Hierro et al., 2007; Seaman et al., 2009). Thus, it is possible that even the wt VPS35 may be able to negatively perturb the function of the retromer when heavily over-expressed.

Regardless of the modes of gene action, the genetic modification of VPS35 can result in the disruption of retromer function and the aberrant trafficking of cargo proteins such as CI-MPR. CI-MPR appears to be the primary receptor for the major lysosomal ' $\alpha$ -synucleinase' CTSD that is abundantly expressed in the brain (Ludwig et al., 1994; Press et al., 1998). Indeed, Sevlever et al. found that the main degradation activity of  $\alpha$ SYN in the lysosomal fractions from cultured neurons was greatly inhibited by the CTSD inhibitor pepstatin A (Sevlever et al., 2008). They showed that other protease inhibitors such as leupeptin weakly reduced  $\alpha$ SYN degradation. This result indicates that in addition to CTSD, other proteolytic activities play a role in  $\alpha$ SYN degradation within lysosomes. This notion is corroborated by our data showing that treatment of the lysosomal inhibitor chloroquine slightly but significantly augmented  $\alpha$ SYN levels in cells transfected with VPS35 siRNA. Nevertheless, the altered processing and prominent accumulation of insoluble species of endogenous  $\alpha$ SYN in three different mammals with CTSD deficiency indicate that its enzyme activity plays a fundamental role in  $\alpha$ SYN metabolism (Cullen et al., 2009). Although both the proteasome and the lysosome have been proposed to play a role in the degradation of  $\alpha$ SYN (Ebrahimi-Fakhari et al., 2011; Konno et al., 2012), recent observations have underscored the contribution of the autophagy-lysosome pathway (Mak et al., 2010; Vogiatzi et al., 2008). CTSD, lysosome-associated membrane protein-1 (LAMP-1), and heat shock protein 73 (Hsp73) immunoreactivities are significantly decreased (approximately 50% versus control) in the substantia nigra neurons of idiopathic PD patients (Chu et al., 2009). Furthermore, parkinsonism has been noted in lysosomal deficiencies such as the adult forms of neuronal ceroid lipofuscinosis, Gaucher disease, and Kufor-Rakeb syndrome (Schneider and Zhang, 2010). The CTSD deficiency is thought to broadly influence the lysosomal and autophagic degradation of its substrate proteins (Koike et al., 2000). Moreover, recent work has revealed that the D620N mutant VPS35 fails to associate with the WASH (Wiskott-Aldrich syndrome protein and SCAR homolog) complex, an important regulator of vesicle trafficking. This failure impairs the autophagic clearance of huntingtin proteins with Q74 repeats and the A53T mutant of  $\alpha$ SYN (Zavodszky et al., 2014), raising the question of how the impaired autophagic-lysosomal degradation by retromer dysfunction can specifically lead to  $\alpha$ SYN accumulation. One possible mechanism is the involvement of the chaperone-mediated autophagy (CMA). Indeed, the amino acid sequence of  $\alpha$ SYN contains a pentapeptide succession consistent with a CMA recognition motif and *in vitro* experiments demonstrated that this motif is essential for the internalization of  $\alpha$ SYN into the lysosomal lumen and for degradation by lysosomal proteases (Cuervo et al., 2004). Another regulatory mechanism which may control the selective sorting and degradation of  $\alpha$ SYN in lysosomes is the ubiquitin-modification. It has been shown that Nedd4 (neural precursor cell expressed developmentally down-regulated protein 4), a ubiquitin E3 ligase that targets protein substrates to lysosomes, catalyzes K63-mediated  $\alpha$ SYN ubiquitination and enhances its clearance in lysosomes (Sugeno et al., 2014; Tofaris et al., 2011). Moreover, the over-expression of wt-Nedd4 reduces  $\alpha$ SYN accumulation in the nervous tissue and induces neurodegeneration and locomotor abnormality in both fly and rat models (Davies et al., 2014). This finding is well corroborated by the yeast model experiment showing that N-aryl benzimidazole (NAB) strongly and selectively counteracts the  $\alpha$ SYN cytotoxicity through its influence on Rsp5, a yeast homolog of Nedd4 (Tardiff et al., 2013). Our experiments using a novel fly model of VPS35-linked PD provide evidence for a modulatory effect of endogenous VPS35 expression on  $\alpha$ SYN toxicity *in vivo*. Despite the lack of direct evidence showing that fruit fly CTSD accepts human  $\alpha$ SYN as a substrate, we found that the knockdown of *dVPS35* significantly

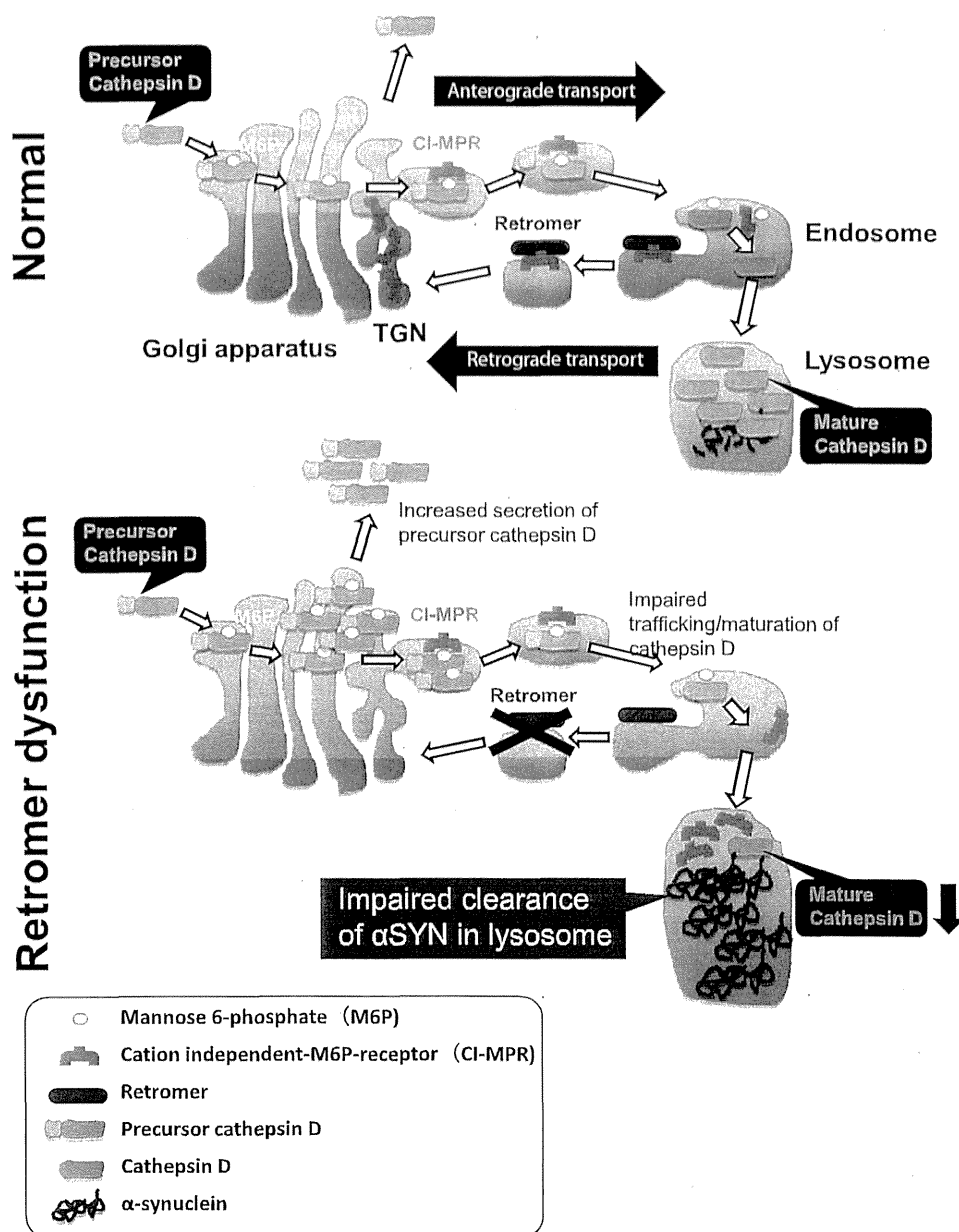


**Fig. 6.** Schematic illustrations of retromer-mediated trafficking of CTSD and possible contribution to lysosomal  $\alpha$ SYN degradation. VPS35, a critical component of the retromer complex, mediates retrograde transport of cargo protein (CI-MPR) from endosome to the TGN. Under physiological condition (upper panel), upon arrival in the Golgi apparatus, newly synthesized CTSD precursor is specifically modified with M6P residues, which are recognized by CI-MPR in the TGN. CI-MPR escorts CTSD into endosomes, in which the CTSD are released for further transport to lysosomes. During this process, CTSD is activated by the proteolytic cleavage of the signal peptide sequence. The retromer retrieves the unoccupied MPRs from endosomes to the TGN, where they participate in further cycles of CTSD sorting. If the retromer function is perturbed (lower panel), the retromer fails to retrieve CI-MPR from the endosome to the TGN, which results in increased secretion of precursor CTSD as well as the impaired trafficking of CTSD. As a consequence, the amount of mature CTSD in the lysosome is decreased, which increases the accumulation of  $\alpha$ SYN and might influence the neurodegenerative process linked to PD.

lowered the CTSD activity in fly brain and the deletion of the homologous CTSD-encoding gene in the fly promoted the toxicity of the ectopically expressed human  $\alpha$ SYN in the fly retina (Cullen et al., 2009). These observations suggest that the altered expression level of dVPS35 may interfere with CTSD activation and thereby have an effect on the cellular burden of  $\alpha$ SYN. Indeed, the accumulation of the HMW Triton-insoluble  $\alpha$ SYN species accompanied by a decrease in soluble monomeric  $\alpha$ SYN in our fly model is consistent with the results in CTSD-deficient mouse brain showing that the level of soluble endogenous  $\alpha$ SYN was reduced, whereas the levels of insoluble, oligomeric  $\alpha$ SYN species were increased (Cullen et al., 2009). The reason that the

$\alpha$ SYN monomer was decreased in the dVPS35-deficient fly brain whereas the monomeric  $\alpha$ SYN was increased in VPS35-silenced HEK293 cells is uncertain. However, it is possible that the long-lasting CTSD deficiency caused by retromer malfunction may facilitate the buildup of the HMW  $\alpha$ SYN species. The eye phenotype of the dVPS35-deficient  $\alpha$ SYN transgenic fly is relatively mild compared to that of CTSD-knockout flies that showed age-dependent vacuolar degeneration and thinning of the retinal architecture (Cullen et al., 2009). Furthermore, the life span of our flies was roughly comparable to that of normal flies, whereas the CTSD-knockdown flies manifested a clearly shortened life span (Tsakiri et al., 2013). Presumably, there may be an inverse

correlation between the severity of the disease and the level of residual CTSD enzyme activity. The observed mild eye degeneration and the age-dependent decline of motor performance in  $\alpha$ SYN Tg flies with a dVPS35-null background may recapitulate the slowly progressive feature of the human disease. Although the underlying molecular mechanism by which VPS35 deficiency facilitates eye disorganization and progressive motor disability in human  $\alpha$ SYN Tg flies remains enigmatic, there is substantial evidence to suggest that the toxic conversion of  $\alpha$ SYN from soluble monomers to aggregated, insoluble forms in the brain is a key event in the pathogenesis of PD and related diseases (Cookson, 2005). Thus, the intracellular buildup of the potentially noxious  $\alpha$ SYN species in the fly brain may partly provide a plausible explanation for the cytotoxicity.

In summary, we found that retromer depletion impaired CTSD maturation in parallel with the accumulation of  $\alpha$ SYN in lysosomes. Moreover, the newly established fly model of VPS35-linked PD provided evidence for a possible modulatory effect of endogenous VPS35 expression on  $\alpha$ SYN toxicity *in vivo*. Interestingly, MacLeod et al. (2013) have demonstrated that wt VPS35 (PARK17) could rescue the phenotypes caused by LRRK2 (PARK8) or RAB7L1 (PARK16) risk variants both *in vitro* and *in vivo*. Furthermore, the locomotor abnormalities and shortened lifespan in flies expressing mutant human LRRK2 can be rescued by the overexpression of VPS35 (Linhart et al., 2014). These findings indicate that these PD-associated genes may configure a common cellular pathway. The functional interrelationship of the endo-lysosomal system in PD is also highlighted by the recent identification of pathogenic mutations in *DNAJC6* and *DNAJC13*, recently identified genes encoding the DNAJ domain-bearing proteins involved in endosomal trafficking, in rare familial forms of PD (Edvardson et al., 2012; Vilarino-Guell et al., 2014). Further studies will be required to gain insight into the pathophysiological role of the endocytosis and endo/lysosomal trafficking systems in synucleinopathy and to identify molecular targets for potential therapeutic interventions.

## Acknowledgments

The authors thank Dr. Matthew J. Farrer (Centre of Applied Neurogenetics, University of British Columbia, Canada) for providing the human wt and mutant (D620N and P316S) VPS35 constructs. This work was supported in part by a Grant-in-Aid for Scientific Research (C) [grant number 26461263], a Grant-in-Aid for Scientific Research (B) [grant number 24390219], and a Grant-in-Aid for Exploratory Research [grant number 24659423] from the Ministry of Education, Culture, Sports, Science and Technology (MEXT); a grant from the Research Committee for Ataxic Diseases, a Grant-in-Aid for Scientific Research on Innovative Areas (Brain Environment) [grant number 24111502] from the Ministry of Health, Labor, and Welfare, Japan; and the Intramural Research Grant [grant number 24–5] for Neurological and Psychiatric Disorders of the National Center of Neurology and Psychiatry (NCNP), Japan.

## References

- Bennett, M.C., Bishop, J.F., Leng, Y., Chock, P.B., Chase, T.N., Mouradian, M.M., 1999. Degradation of alpha-synuclein by proteasome. *J. Biol. Chem.* 274, 33855–33858.
- Capony, F., Rougeot, C., Montcourrier, P., Cavailles, V., Salazar, C., Rochefort, H., 1989. Increased secretion, altered processing, and glycosylation of pro-cathepsin D in human mammary cancer cells. *Cancer Res.* 49, 3904–3909.
- Chen, L., Feany, M.B., 2005. Alpha-synuclein phosphorylation controls neurotoxicity and inclusion formation in a *Drosophila* model of Parkinson disease. *Nat. Neurosci.* 8, 657–663.
- Chu, Y., Dodiya, H., Aebischer, P., Olanow, C.W., Kordower, J.H., 2009. Alterations in lysosomal and proteasomal markers in Parkinson's disease: relationship to alpha-synuclein inclusions. *Neurobiol. Dis.* 35, 385–398.
- Cookson, M.R., 2005. The biochemistry of Parkinson's disease. *Annu. Rev. Biochem.* 74, 29–52.
- Cuervo, A.M., Stefanis, L., Fredenburg, R., Lansbury, P.T., Sulzer, D., 2004. Impaired degradation of mutant alpha-synuclein by chaperone-mediated autophagy. *Science* 305, 1292–1295.

- Cullen, V., Lindfors, M., Ng, J., Paetau, A., Swinton, E., Kolodziej, P., Boston, H., Saftig, P., Woulfe, J., Feany, M.B., Myllykangas, L., Schlossmacher, M.G., Tyynela, J., 2009. Cathepsin D expression level affects alpha-synuclein processing, aggregation, and toxicity *in vivo*. *Mol. Brain* 2, 5.
- Davies, S.E., Hallett, P.J., Moens, T., Smith, G., Mangano, E., Kim, H.T., Goldberg, A.L., Liu, J.L., Isacson, O., Tofaris, G.K., 2014. Enhanced ubiquitin-dependent degradation by Nedd4 protects against alpha-synuclein accumulation and toxicity in animal models of Parkinson's disease. *Neurobiol. Dis.* 64, 79–87.
- Dehay, B., Martinez-Vicente, M., Caldwell, G.A., Caldwell, K.A., Yue, Z., Cookson, M.R., Klein, C., Vila, M., Bezdard, E., 2013. Lysosomal impairment in Parkinson's disease. *Mov. Disord.* 28, 725–732.
- Ebrahimi-Fakhari, D., Cantuti-Castelvetri, I., Fan, Z., Rockenstein, E., Masliah, E., Hyman, B.T., McLean, P.J., Unni, V.K., 2011. Distinct roles *in vivo* for the ubiquitin–proteasome system and the autophagy–lysosomal pathway in the degradation of alpha-synuclein. *J. Neurosci.* 31, 14508–14520.
- Edvardson, S., Cinnamon, Y., Ta-Shma, A., Shaag, A., Yim, Y.I., Zenvirt, S., Jalas, C., Lesage, S., Brice, A., Taraboulos, A., Kaestner, K.H., Greene, L.E., Elpeleg, O., 2012. A deleterious mutation in *DNAJC6* encoding the neuronal-specific clathrin-uncoating co-chaperone auxilin, is associated with juvenile parkinsonism. *PLoS One* 7, e36458.
- Feany, M.B., Bender, W.W., 2000. A *Drosophila* model of Parkinson's disease. *Nature* 404, 394–398.
- Follett, J., Norwood, S.J., Hamilton, N.A., Mohan, M., Kovtun, O., Tay, S., Zhe, Y., Wood, S.A., Mellick, G.D., Silburn, P.A., Collins, B.M., Bugarcic, A., Teasdale, R.D., 2014. The Vps35 D620N mutation linked to Parkinson's disease disrupts the cargo sorting function of retromer. *Traffic* 15, 230–244.
- Hasegawa, T., Matsuzaki, M., Takeda, A., Kikuchi, A., Akita, H., Perry, G., Smith, M.A., Itoyama, Y., 2004. Accelerated alpha-synuclein aggregation after differentiation of SH-SY5Y neuroblastoma cells. *Brain Res.* 1013, 51–59.
- Hasegawa, T., Matsuzaki-Kobayashi, M., Takeda, A., Sugeno, N., Kikuchi, A., Furukawa, K., Perry, G., Smith, M.A., Itoyama, Y., 2006. Alpha-synuclein facilitates the toxicity of oxidized catechol metabolites: implications for selective neurodegeneration in Parkinson's disease. *FEBS Lett.* 580, 2147–2152.
- Hasegawa, T., Baba, T., Kobayashi, M., Konno, M., Sugeno, N., Kikuchi, A., Itoyama, Y., Takeda, A., 2010. Role of TPPP/p25 on alpha-synuclein-mediated oligodendroglial degeneration and the protective effect of SIRT2 inhibition in a cellular model of multiple system atrophy. *Neurochem. Int.* 57, 857–866.
- Hasegawa, T., Konno, M., Baba, T., Sugeno, N., Kikuchi, A., Kobayashi, M., Miura, E., Tanaka, N., Tamai, K., Furukawa, K., Arai, H., Mori, F., Wakabayashi, K., Aoki, M., Itoyama, Y., Takeda, A., 2011. The AAA-ATPase VPS4 regulates extracellular secretion and lysosomal targeting of alpha-synuclein. *PLoS One* 6, e29460.
- Hierro, A., Rojas, A.L., Rojas, R., Murthy, N., Effantini, G., Kajava, A.V., Steven, A.C., Bonifacino, J. S., Hurley, J.H., 2007. Functional architecture of the retromer cargo-recognition complex. *Nature* 449, 1063–1067.
- Hilgers, V., Bushati, N., Cohen, S.M., 2010. *Drosophila* microRNAs 263a/b confer robustness during development by protecting nascent sense organs from apoptosis. *PLoS Biol.* 8, e1000396.
- Koike, M., Nakanishi, H., Saftig, P., Ezaki, J., Ishihara, K., Ohsawa, Y., Schulz-Schaeffer, W., Watanaka, T., Waguri, S., Kametaka, S., Shibata, M., Yamamoto, K., Kominami, E., Peters, C., von Figura, K., Uchiyama, Y., 2000. Cathepsin D deficiency induces lysosomal storage with ceroid lipofuscin in mouse CNS neurons. *J. Neurosci.* 20, 6898–6906.
- Konno, M., Hasegawa, T., Baba, T., Miura, E., Sugeno, N., Kikuchi, A., Fiesel, F.C., Sasaki, T., Aoki, M., Itoyama, Y., Takeda, A., 2012. Suppression of dynamin GTPase decreases alpha-synuclein uptake by neuronal and oligodendroglial cells: a potent therapeutic target for synucleinopathy. *Mol. Neurodegener.* 7, 38.
- Korolchuk, V.I., Schutz, M.M., Gomez-Llorente, C., Rocha, J., Lansu, N.R., Collins, S.M., Waitkar, Y.P., Robinson, I.M., O'Kane, C.J., 2007. *Drosophila* Vps35 function is necessary for normal endocytic trafficking and actin cytoskeleton organization. *J. Cell Sci.* 120, 4367–4376.
- Laurent-Matha, V., Derocq, D., Prebois, C., Katunuma, N., Liudet-Coopman, E., 2006. Processing of human cathepsin D is independent of its catalytic function and auto-activation: involvement of cathepsins L and B. *J. Biochem.* 139, 363–371.
- Lee, B.R., Kamitani, T., 2011. Improved immunodetection of endogenous alpha-synuclein. *PLoS One* 6, e23939.
- Linhart, R., Wong, S.A., Cao, J., Tran, M., Huynh, A., Ardrey, C., Park, J.M., Hsu, C., Taha, S., Peterson, R., Shea, S., Kurian, J., Venderova, K., 2014. Vacuolar protein sorting 35 (Vps35) rescues locomotor deficits and shortened lifespan in *Drosophila* expressing a Parkinson's disease mutant of Leucine-rich repeat kinase 2 (LRRK2). *Mol. Neurodegener.* 9, 23.
- Ludwig, T., Munier-Lehmann, H., Bauer, U., Hollinshead, M., Ovitt, C., Lobel, P., Hoflack, B., 1994. Differential sorting of lysosomal enzymes in mannose 6-phosphate receptor-deficient fibroblasts. *EMBO J.* 13, 3430–3437.
- MacLeod, D.A., Rhinn, H., Kuwahara, T., Zolin, A., Di Paolo, G., McCabe, B.D., Marder, K.S., Honig, L.S., Clark, L.N., Small, S.A., Abeliovich, A., 2013. RAB7L1 interacts with LRRK2 to modify intraneuronal protein sorting and Parkinson's disease risk. *Neuron* 77, 425–439.
- Mak, S.K., McCormack, A.L., Manning-Bog, A.B., Cuervo, A.M., Di Monte, D.A., 2010. Lysosomal degradation of alpha-synuclein *in vivo*. *J. Biol. Chem.* 285, 13621–13629.
- Muhammad, A., Flores, I., Zhang, H., Yu, R., Staniszewski, A., Planell, E., Herman, M., Ho, L., Kreber, R., Honig, L.S., Ganetzky, B., Duff, K., Arancio, O., Small, S.A., 2008. Retromer deficiency observed in Alzheimer's disease causes hippocampal dysfunction, neurodegeneration, and Abeta accumulation. *Proc. Natl. Acad. Sci. U. S. A.* 105, 7327–7332.
- Poewe, W., Mahlknecht, P., 2009. The clinical progression of Parkinson's disease. *Parkinsonism Relat. Disord.* 15 (Suppl. 4), S28–S32.
- Press, B., Feng, Y., Hoflack, B., Wandinger-Ness, A., 1998. Mutant Rab7 causes the accumulation of cathepsin D and cation-independent mannose 6-phosphate receptor in an early endocytic compartment. *J. Cell Biol.* 140, 1075–1089.

- Rojas, R., van Vlijmen, T., Mardones, G.A., Prabhu, Y., Rojas, A.L., Mohammed, S., Heck, A.J., Raposo, G., van der Sluijs, P., Bonifacino, J.S., 2008. Regulation of retromer recruitment to endosomes by sequential action of Rab5 and Rab7. *J. Cell Biol.* 183, 513–526.
- Schneider, L., Zhang, J., 2010. Lysosomal function in macromolecular homeostasis and bioenergetics in Parkinson's disease. *Mol. Neurodegener.* 5, 14.
- Seaman, M.N., 2004. Cargo-selective endosomal sorting for retrieval to the Golgi requires retromer. *J. Cell Biol.* 165, 111–122.
- Seaman, M.N., Marcussan, E.G., Cereghino, J.L., Emr, S.D., 1997. Endosome to Golgi retrieval of the vacuolar protein sorting receptor, Vps10p, requires the function of the VPS29, VPS30, and VPS35 gene products. *J. Cell Biol.* 137, 79–92.
- Seaman, M.N., Harbour, M.E., Tattersall, D., Read, E., Bright, N., 2009. Membrane recruitment of the cargo-selective retromer subcomplex is catalysed by the small GTPase Rab7 and inhibited by the Rab-GAP TBC1D5. *J. Cell Sci.* 122, 2371–2382.
- Sevlever, D., Jiang, P., Yen, S.H., 2008. Cathepsin D is the main lysosomal enzyme involved in the degradation of alpha-synuclein and generation of its carboxy-terminally truncated species. *Biochemistry* 47, 9678–9687.
- Singleton, A.B., Farrer, M.J., Bonifati, V., 2013. The genetics of Parkinson's disease: progress and therapeutic implications. *Mov. Disord.* 28, 14–23.
- Small, S.A., Kent, K., Pierce, A., Leung, C., Kang, M.S., Okada, H., Honig, L., Vonsattel, J.P., Kim, T.W., 2005. Model-guided microarray implicates the retromer complex in Alzheimer's disease. *Ann. Neurol.* 58, 909–919.
- Spillantini, M.G., Schmidt, M.L., Lee, V.M., Trojanowski, J.Q., Jakes, R., Goedert, M., 1997. Alpha-synuclein in Lewy bodies. *Nature* 388, 839–840.
- Springer, W., Kahle, P.J., 2011. Regulation of PINK1-Parkin-mediated mitophagy. *Autophagy* 7, 266–278.
- Sugeno, N., Takeda, A., Hasegawa, T., Kobayashi, M., Kikuchi, A., Mori, F., Wakabayashi, K., Itoyama, Y., 2008. Serine 129 phosphorylation of alpha-synuclein induces unfolded protein response-mediated cell death. *J. Biol. Chem.* 283, 23179–23188.
- Sugeno, N., Hasegawa, T., Tanaka, N., Fukuda, M., Wakabayashi, K., Oshima, R., Konno, M., Miura, E., Kikuchi, A., Baba, T., Anan, T., Nakao, M., Geisler, S., Aoki, M., Takeda, A., 2014. K63-linked ubiquitination by E3 ubiquitin ligase Nedd4-1 facilitates endosomal sequestration of internalized alpha-synuclein. *J. Biol. Chem.* 289, 18137–18151.
- Tardiff, D.F., Jui, N.T., Khurana, V., Tambe, M.A., Thompson, M.L., Chung, C.Y., Kamadurai, H.B., Kim, H.T., Lancaster, A.K., Caldwell, K.A., Caldwell, G.A., Rochet, J.C., Buchwald, S.L., Lindquist, S., 2013. Yeast reveal a "druggable" Rsp5/Nedd4 network that ameliorates alpha-synuclein toxicity in neurons. *Science* 342, 979–983.
- Tofaris, G.K., 2012. Lysosome-dependent pathways as a unifying theme in Parkinson's disease. *Mov. Disord.* 27, 1364–1369.
- Tofaris, G.K., Kim, H.T., Hourez, R., Jung, J.W., Kim, K.P., Goldberg, A.L., 2011. Ubiquitin ligase Nedd4 promotes alpha-synuclein degradation by the endosomal-lysosomal pathway. *Proc. Natl. Acad. Sci. U. S. A.* 108, 17004–17009.
- Tsakiri, E.N., Iliaki, K.K., Hohn, A., Grimm, S., Papassideri, I.S., Grune, T., Trougakos, I.P., 2013. Diet-derived advanced glycation end products or lipofuscin disrupts proteostasis and reduces life span in *Drosophila melanogaster*. *Free Radic. Biol. Med.* 65c, 1155–1163.
- Tsika, E., Glauser, L., Moser, R., Fiser, A., Daniel, G., Sheerin, U.M., Lees, A., Troncoso, J.C., Lewis, P.A., Bandopadhyay, R., Schneider, B.L., Moore, D.J., 2014. Parkinson's disease-linked mutations in VPS35 induce dopaminergic neurodegeneration. *Hum. Mol. Genet.* 23, 4621–4638.
- Vilarino-Guell, C., Wider, C., Ross, O.A., Dachselt, J.C., Kachergus, J.M., Lincoln, S.J., Soto-Ortolaza, A.L., Cobb, S.A., Wilhoite, G.J., Bacon, J.A., Behrouz, B., Melrose, H.L., Hentati, E., Puschmann, A., Evans, D.M., Conibear, E., Wasserman, W.W., Aasly, J.O., Burkhard, P.R., Djaldetti, R., Chika, J., Hentati, F., Krygowska-Wajs, A., Lynch, T., Melamed, E., Rajput, A., Rajput, A.H., Solida, A., Wu, R.M., Uitti, R.J., Wszolek, Z.K., Vingerhoets, F., Farrer, M.J., 2011. VPS35 mutations in Parkinson disease. *Am. J. Hum. Genet.* 89, 162–167.
- Vilarino-Guell, C., Rajput, A., Milnerwood, A.J., Shah, B., Szu-Tu, C., Trinh, J., Yu, I., Encarnacion, M., Munsie, L.N., Tapia, L., Gustavsson, E.K., Chou, P., Tatarnikov, I., Evans, D.M., Pishotta, F.T., Volta, M., Beccano-Kelly, D., Thompson, C., Lin, M.K., Sherman, H.E., Han, H.J., Guenther, B.L., Wasserman, W.W., Bernard, V., Ross, C.J., Appel-Cresswell, S., Stoessl, A.J., Robinson, C.A., Dickson, D.W., Ross, O.A., Wszolek, Z.K., Aasly, J.O., Wu, R.M., Hentati, F., Gibson, R.A., McPherson, P.S., Girard, M., Rajput, M., Rajput, A.H., Farrer, M.J., 2014. DNAJC13 mutations in Parkinson disease. *Hum. Mol. Genet.* 23, 1794–1801.
- Vogiatzi, T., Xilouri, M., Vekrellis, K., Stefanis, L., 2008. Wild type alpha-synuclein is degraded by chaperone-mediated autophagy and macroautophagy in neuronal cells. *J. Biol. Chem.* 283, 23542–23556.
- Wales, P., Pinho, R., Lazaro, D.F., Outeiro, T.F., 2013. Limelight on alpha-synuclein: pathological and mechanistic implications in neurodegeneration. *J. Parkinsons Dis.* 3, 415–459.
- Wen, L., Tang, F.L., Hong, Y., Luo, S.W., Wang, C.L., He, W., Shen, C., Jung, J.U., Xiong, F., Lee, D.H., Zhang, Q.G., Brann, D., Kim, T.W., Yan, R., Mei, L., Xiong, W.C., 2011. VPS35 haploinsufficiency increases Alzheimer's disease neuropathology. *J. Cell Biol.* 195, 765–779.
- Yamaguchi, M., Hirose, F., Inoue, Y.H., Shiraki, M., Hayashi, Y., Nishi, Y., Matsukage, A., 1999. Ectopic expression of human p53 inhibits entry into S phase and induces apoptosis in the *Drosophila* eye imaginal disc. *Oncogene* 18, 6767–6775.
- Zavodszky, E., Seaman, M.N., Moreau, K., Jimenez-Sanchez, M., Breusegem, S.Y., Harbour, M.E., Rubinsztein, D.C., 2014. Mutation in VPS35 associated with Parkinson's disease impairs WASH complex association and inhibits autophagy. *Nat. Commun.* 5, 3828.
- Zhao, X., Nothwehr, S., Lara-Lemus, R., Zhang, B.Y., Peter, H., Arvan, P., 2007. Dominant-negative behavior of mammalian Vps35 in yeast requires a conserved PRLYL motif involved in retromer assembly. *Traffic* 8, 1829–1840.
- Zimprich, A., Benet-Pages, A., Struhal, W., Graf, E., Eck, S.H., Offman, M.N., Haubenberger, D., Spielberger, S., Schulte, E.C., Lichtner, P., Rossle, S.C., Klopp, N., Wolf, E., Seppi, K., Pirker, W., Presslauer, S., Mollenhauer, B., Katzenschlager, R., Foki, T., Hotzy, C., Reinthaler, E., Harutyunyan, A., Kralovics, R., Peters, A., Zimprich, F., Brucke, T., Poewe, W., Auff, E., Trenkwalder, C., Rost, B., Ransmayr, G., Winkelmann, J., Meitinger, T., Strom, T.M., 2011. A mutation in VPS35, encoding a subunit of the retromer complex, causes late-onset Parkinson disease. *Am. J. Hum. Genet.* 89, 168–175.

# Lys-63-linked Ubiquitination by E3 Ubiquitin Ligase Nedd4-1 Facilitates Endosomal Sequestration of Internalized $\alpha$ -Synuclein\*

Received for publication, April 1, 2014, and in revised form, May 11, 2014. Published, JBC Papers in Press, May 15, 2014, DOI 10.1074/jbc.M113.529461

Naoto Sugeno<sup>‡</sup>, Takafumi Hasegawa<sup>†1</sup>, Nobuyuki Tanaka<sup>§</sup>, Mitsunori Fukuda<sup>¶</sup>, Koichi Wakabayashi<sup>||</sup>, Ryuji Oshima<sup>§§</sup>, Masashi Konno<sup>‡</sup>, Emiko Miura<sup>‡</sup>, Akio Kikuchi<sup>‡</sup>, Toru Baba<sup>‡</sup>, Tadashi Anan<sup>\*\*</sup>, Mitsuyoshi Nakao<sup>††</sup>, Sven Geisler<sup>§§</sup>, Masashi Aoki<sup>‡</sup>, and Atsushi Takeda<sup>‡2</sup>

From the <sup>‡</sup>Division of Neurology, Department of Neuroscience and Sensory Organs, Tohoku University Graduate School of Medicine, Sendai 980-8574, Japan, the <sup>§</sup>Division of Cancer Biology and Therapeutics, Miyagi Cancer Center Research Institute, Natori 981-1293, Japan, the <sup>¶</sup>Laboratory of Membrane Trafficking Mechanisms, Department of Developmental Biology and Neurosciences, Graduate School of Life Sciences, Tohoku University, Sendai 980-8578, Japan, the <sup>||</sup>Department of Neuropathology, Institute of Brain Science, Hirosaki University School of Medicine, Hirosaki 036-8562, Japan, the <sup>\*\*</sup>Department of Pediatrics, Kumamoto University School of Medicine, Kumamoto 860-0811, Japan, the <sup>††</sup>Department of Medical Cell Biology, Institute of Molecular Embryology and Genetics, Kumamoto University, Kumamoto 860-0811, Japan, and the <sup>§§</sup>Laboratory of Functional Neurogenetics, Department for Neurodegenerative Diseases, Hertie Institute for Clinical Brain Research, University of Tübingen, German Centre for Neurodegenerative Diseases, Tübingen 72076, Germany

**Background:** Nedd4-1 catalyzes the Lys-63-linked ubiquitination of aS.

**Results:** The Lys-63-linked ubiquitination of aS by Nedd4-1 facilitates endosomal targeting of extracellular aS.

**Conclusion:** Compared with C-terminal deficient mutants, wild type-aS is preferentially internalized and translocates to endosomes. The overexpression of Nedd4-1 leads to the accumulation of aS in endosomes.

**Significance:** Nedd4-1-mediated Lys-63 ubiquitination specifies the fate of internalized aS.

$\alpha$ -Synuclein (aS) is a major constituent of Lewy bodies, which are not only a pathological marker for Parkinson disease but also a trigger for neurodegeneration. Cumulative evidence suggests that aS spreads from cell to cell and thereby propagates neurodegeneration to neighboring cells. Recently, Nedd4-1 (neural precursor cell expressed developmentally down-regulated protein 4-1), an E3 ubiquitin ligase, was shown to catalyze the Lys-63-linked polyubiquitination of intracellular aS and thereby facilitate aS degradation by the endolysosomal pathway. Because Nedd4-1 exerts its activity in close proximity to the inner leaflet of the plasma membrane, we speculate that after the internalization of aS the membrane resident aS is preferentially ubiquitinated by Nedd4-1. To clarify the role of Nedd4-1 in aS internalization and endolysosomal sequestration, we generated aS mutants, including  $\Delta$ PR1(1–119 and 129–140),  $\Delta$ C(1–119), and  $\Delta$ PR2(1–119 and 134–140), that lack the proline-rich sequence, a putative Nedd4-1 recognition site. We show that wild type aS, but not  $\Delta$ PR1,  $\Delta$ PR2, or  $\Delta$ C aS, is modified by Nedd4-1 *in vitro*, acquiring a Lys-63-linked ubiquitin chain. Compared with the mutants lacking the proline-rich sequence,

wild type-aS is preferentially internalized and translocated to endosomes. The overexpression of Nedd4-1 increased aS in endosomes, whereas RNAi-mediated silencing of Nedd4-1 decreased endosomal aS. Although aS freely passes through plasma membranes within minutes, a pulse-chase experiment revealed that the overexpression of Nedd4-1 markedly decreased the re-secretion of internalized aS. Together, these findings demonstrate that Nedd4-1-linked Lys-63 ubiquitination specifies the fate of extrinsic and *de novo* synthesized aS by facilitating their targeting to endosomes.

The intraneuronal aggregation of misfolded  $\alpha$ -synuclein (aS),<sup>3</sup> known as a component of Lewy bodies (LB), is a pathological hallmark of Parkinson disease (PD). After the discovery of LB-like inclusions in the grafted neurons of PD patients who had previously received transplants of fetal mesencephalic neurons (1), increasing evidence has suggested that both monomeric and oligomeric aS can be secreted into the extracellular milieu (2), thereby affecting the physiological state of neighboring cells. Previous studies have revealed that the cellular uptake of fibrillar aS requires physiological temperatures and dynamin-1 (3, 4), a master regulator of endocytic vesicle formation, suggesting the

\* This work was supported in part by Grants-in-aid for Scientific Research (C) 25461264 and 23591228, Grant-in-aid for Scientific Research (B) 24390219, Grant-in-aid for Exploratory Research 24659423, Grant-in-aid for Scientific Research on Innovative Areas (Brain Environment) 24111502 from the Ministry of Education, Culture, Sports, Science and Technology, a grant from the Research Committee for Ataxic Diseases, the Ministry of Health, Labor, and Welfare, Japan, a grant from the Symposium on Catecholamine and Neurological Disorders, and a grant from the 17th Takeda Science Foundation Symposium on Bioscience.

<sup>1</sup> To whom correspondence should be addressed. Tel.: 81-22-717-7189; Fax: 81-22-717-7192; E-mail: thasegawa@med.tohoku.ac.jp.

<sup>2</sup> Present address: Dept. of Neurology, National Hospital Organization, Sendai-Nishitaga Hospital, Sendai 982-8555, Japan.

<sup>3</sup> The abbreviations used are: aS,  $\alpha$ -synuclein; CQ, chloroquine; HECT, homologous to the E6-AP C terminus; HMW, high molecular weight; LB, Lewy body; LMW, low molecular weight; Nedd4, neural precursor cell expressed developmentally down-regulated protein 4; pAb, polyclonal antibody; PD, Parkinson disease; PR, proline-rich; aS,  $\alpha$ -synuclein; Tricine, N-[2-hydroxy-1,1-bis(hydroxymethyl)ethyl]glycine; ESCRT, endosomal sorting complex required for transport; BN, blue native.

## Nedd4-1 Targets Internalized $\alpha$ -Synuclein to Endosomes

active participation of the endocytic machinery. However,  $\alpha$ S incorporation into cells is not completely disabled by the inhibition of endocytosis (3), indicating that other pathways, such as direct penetration, macropinocytosis, pore formation, and diffusion, might be involved in  $\alpha$ S internalization (5). This notion is supported by previous studies showing that both monomers and oligomers of  $\alpha$ S can freely pass through plasma membranes (4).

Because the aggregated  $\alpha$ S in the brains of PD patients is robustly ubiquitinated (6–8), the ubiquitin modification of  $\alpha$ S may regulate the biogenesis of LBs and could contribute to neurodegeneration in PD. Among the E3 ligases that catalyze  $\alpha$ S ubiquitination, researchers have focused on Nedd4 (neural precursor cell expressed developmentally down-regulated protein 4) because this E3 ligase is highly expressed in neurons containing LBs and catalyzes the Lys-63-linked ubiquitination of  $\alpha$ S (9, 10). Mammalian Nedd4 exists in two isoforms, Nedd4-1 and Nedd4-2. Structurally, the Nedd4 isoforms are composed of a C2 domain, 3–4 WW domains, which recognize proline-rich motifs (PPXY or LPXY) in substrate proteins (11, 12), and a catalytic domain homologous to the E6-AP C-terminal (HECT) domain at the C terminus. Nedd4-1 binds to the plasma membrane via the C2 domain in a  $\text{Ca}^{2+}$ -dependent manner (13) and controls the ubiquitination of membrane-bound receptor proteins, such as the epithelial  $\text{Na}^+$  channel (11). Modification by Lys-63-linked ubiquitination promotes the sorting of receptors for endocytosis and their subsequent degradation through the endolysosomal pathway (14). Given that Nedd4-1 exerts its E3 ligase activity in close proximity to the inner leaflet of the plasma membrane, the catalytic activity of Nedd4-1 likely acts preferentially on membrane-resident  $\alpha$ S. In this study, we explored the possible mechanism by which the ubiquitination of  $\alpha$ S by Nedd4-1 in the juxtamembrane cytoplasm could contribute to the incorporation and endosomal targeting of  $\alpha$ S.

### EXPERIMENTAL PROCEDURES

**Cell Culture, Plasmid Preparation, and Transfection**—SH-SY5Y human dopaminergic neuroblastoma cells (ATCC, Manassas, VA) were maintained in DMEM (Invitrogen) supplemented with 10% FBS (Thermo Scientific, MA) at 37 °C under humidified 5%  $\text{CO}_2$ /air. Triple FLAG-tagged human wild type Nedd4-1 was subcloned into the CMV10 vector. The HECT active-site dead mutant, C867A, and WW1–4-deleted ( $\Delta$ WW) mutant were produced by PCR-based *in vitro* mutagenesis. The pEGFP-C1 plasmids encoding enhanced GFP-tagged human wild type-Rab5a, wild type-Rab7, and wild type-Rab11a were described previously (2). The DNA plasmids were isolated and purified using the GenoPure plasmid maxi kit (Roche Applied Science).  $1 \times 10^6$  cells were transfected with 5  $\mu\text{g}$  of plasmid DNA using the NEPA21 square wave electroporator (Nepa Gene, Chiba, Japan).

**Recombinant Protein Purification**—After the GST-wild type- $\alpha$ S(1–140) fusion construct was subcloned into the pGEX-6P-1 bacterial expression vector, the  $\Delta$ PR1(1–119 and 129–140),  $\Delta$ PR2(1–119 and 134–140),  $\Delta$ C(1–119), P120A, P128A, and S129A  $\alpha$ S constructs were produced using the PrimeSTAR<sup>®</sup> mutagenesis basal kit (TaKaRa, Otsu, Japan). All recombinant proteins were expressed in the BL21(DE3)pLysS *Escherichia coli* strain and purified as described previously (3). The purity

and identity of the recombinant proteins were verified by Coomassie Brilliant Blue (MP Biomedicals, OH) staining and Western blot analysis. To verify the native state of recombinant  $\alpha$ S, proteins were separated by blue native-PAGE (BN-PAGE). Briefly, the samples were charged by BN sample buffer (50 mM imidazole, pH 7.0, 50 mM NaCl, 5 mM 6-aminohexanoic acid, 0.5% Coomassie G-250, 1.0% digitonin, 20% glycerol) and then subjected to Any-KD<sup>™</sup> TGX<sup>™</sup> gradient gel (Invitrogen) with cathode buffer (0.02% Coomassie G-250, 50 mM Tricine, 7.5 mM imidazole, pH 7.0) and anode buffer (25 mM imidazole, pH 7.0). The proteins were electrophoresed for 20 min at 200 V, 4 °C, followed by a change of the Coomassie G-250 concentration of the cathode buffer to 0.002%, electrophoresis was continued for 60 min at 200 V, and then electroblotted onto a PVDF membrane.

**In Vitro and in Vivo Ubiquitination Assays**—The *in vitro* ubiquitination assay was performed according to the manufacturer's instructions (Enzo Life Sciences, New York). Briefly, 10 nM recombinant  $\alpha$ S and 0.5  $\mu\text{g}$  per reaction of the E3 ubiquitin ligase (E3) described below were incubated with 125 nM biotinylated ubiquitin, 5 nM E1 ubiquitin-activating enzyme (E1), 250 nM E2 ubiquitin-conjugating enzyme (E2), 250  $\mu\text{M}$  Mg-ATP, and 10 units/ml inorganic pyrophosphatase (Sigma) at 37 °C for 30 min, and the reaction was quenched with 2 $\times$  Laemmli buffer. All materials other than E3 and inorganic pyrophosphatase were obtained from Enzo Life Sciences. The E2s used were as follows: UbcH1, UbcH2, UbcH3, UbcH5a, UbcH5b, UbcH5c, UbcH6, UbcH7, UbcH8, UbcH10, and UbcH13/Mms2 (Enzo Life Sciences). The E3s used were as follows: SIAH-1 (Abnova, Taipei, Taiwan), SIAH-2 (Abnova), CHIP (Millipore), Hsp70 (Enzo Life Sciences), E6-AP (Boston-Biochem), Nedd4-1 (Abcam), and Nedd4-2 (Abnova).

**RNAi Interference**—To ablate Nedd4 expression in cultured cells, siRNA specifically targeting human Nedd4-1 (sc-41079, Santa Cruz Biotechnology) or Nedd4-2 (NEDD4LHSS118599, Invitrogen) or a scrambled control siRNA (sc-36869, Santa Cruz Biotechnology) was used. To silence human CHMP2B, a target-specific siRNA (sc-72895, Santa Cruz Biotechnology) was used. For human  $\alpha$ S silencing, a 25-nucleotide-long siRNA was used, 5'-GACCAAAGAGCAAGUGACAAAUGUU-3' (BONAC, Kurume, Japan) (15). SH-SY5Y cells in log phase growth were transfected with target-specific or control-scrambled siRNAs by electroporation. Then 24 h after gene silencing, 5  $\mu\text{M}$  recombinant  $\alpha$ S was added to the culture media, and the cells were incubated for another 24 h.

**Subcellular Fractionation**—For the subcellular fractionation of cultured cells, we adopted an established protocol (16). After being cultured for 24 h in medium containing 5  $\mu\text{M}$   $\alpha$ S, the cells ( $1 \times 10^7$ ) were resuspended in 1 ml of ice-cold buffer (10 mM Tris/acetic acid, pH 7.0, and 250 mM sucrose) and homogenized using 20 strokes in a 2-ml Dounce tissue grinder. In some experiments, the cells were pretreated with 5  $\mu\text{M}$  chloroquine (CQ, Sigma) and/or 10  $\mu\text{M}$  MG132 (Millipore/Calbiochem) before exposure to  $\alpha$ S. The cell homogenate was initially cleared by centrifugation (4000  $\times g$  for 2 min) to remove debris, undestroyed cells, plasma membrane, and nuclei. The supernatant was ultracentrifuged at 100,000  $\times g$  (Hitachi Koki Co., Ltd., Tokyo, Japan) for 2 min to pellet the mitochondria, endosomes,



## Nedd4-1 Targets Internalized $\alpha$ -Synuclein to Endosomes

and lysosomes (fraction EL). Lysosomes were isolated from fraction EL by osmotic lysis for 10 min using a 5:1 ratio (v/v) of pellet to water. After another centrifugation step at  $100,000 \times g$  for 2 min, the lysosomal proteins were recovered in the supernatant, and the mitochondria and endosomes remained in the pellet. The total protein in the culture media was extracted by trichloroacetic acid (TCA)/acetone precipitation and dissolved in 8 M urea, 5% SDS with sonication (2).

**Western Blot Analysis**—After measuring the protein concentration using a bicinchoninic acid protein assay kit (Thermo Scientific), lysates containing 20  $\mu$ g of protein were electrophoresed, and the separated proteins were then electroblotted onto a PVDF membrane. After blocking with TBST containing 5% nonfat dry milk, the membranes were incubated with the following: anti-FLAG/M2 mouse monoclonal Ab (mAb) (1:1000, Sigma); anti-HA mouse mAb (1:1000, CST); anti-synuclein-1 mouse mAb (1:1000, BD Biosciences); anti-aS rabbit polyclonal Ab (pAb) (2628; 1:1000, CST); anti-aS mouse mAb (Syn211; 1:1000, Sigma); anti-SIAH-1 rabbit pAb (1:1000, Abnova); anti-SIAH-2 rabbit pAb (1:1000, Sigma); anti-CHIP rabbit pAb (1:1000, Santa Cruz Biotechnology); anti-Hsp70 (1:1000, StressGen); anti-E6AP mouse mAb (1:1000, Enzo Life Sciences); anti-Nedd4-1 rabbit pAb (1:1000, Abcam); anti-Nedd4-2 rabbit pAb (1:1000, CST); anti-BSA polyclonal Ab (1:2000, Santa Cruz Biotechnology); anti-Hsp90 mouse mAb (1:4000, StressGen); anti-ubiquitin Ab (P4D1; 1:1000, Santa Cruz Biotechnology); anti-Rab7 rabbit pAb (1:1000, CST); and anti-LAMP-2 mouse mAb (H4B4; 1:1000, DSHB). The primary antibodies were followed by HRP-conjugated secondary Ab (1:10,000, Jackson ImmunoResearch). The bands were visualized with the Luminata<sup>TM</sup> Forte Western HRP substrate (Millipore), and the images were captured using the Omega Lum G imaging system (Aplegen, Pleasanton, CA). All experiments were performed at least three times, and each of the bands was digitalized using ImageJ software (National Institutes of Health). Differences between the conditions were analyzed with Dunnett's multiple comparisons test using GraphPad Prism, version 6, for Mac OS X (GraphPad Software). The data are expressed as the means  $\pm$  S.E.

**Immunocytochemistry and Confocal Laser Scanning Microscopy**—Recombinant aS was labeled with Alexa Fluor 488 or Alexa Fluor 555 reactive fluorescent dyes with tetrafluorophenyl ester binding (Invitrogen). Unattached dyes were carefully removed by size exclusion chromatography using Bio-Gel P-6 (Bio-Rad). Twenty four hours before the treatment with fluorophore-labeled aS (5  $\mu$ M, 24 h), enhanced GFP-tagged Rab5a, Rab7, or Rab11a (markers for early, late, or recycling endosomes, respectively) was transfected into the SH-SY5Y cells. In some experiments, GFP-tagged human p62 expression constructs based on the baculovirus backbone (Premo Autophagy Sensors, Invitrogen) were co-transfected 16 h prior to the microscopic observation. To visualize lysosomes or mitochondria, the cells were treated with 100 nM LysoTracker<sup>®</sup> Green or 100 nM MitoTracker<sup>®</sup> Green for 30 min.

The cells were fixed in 4% (w/v) paraformaldehyde in phosphate-buffered saline (PBS) for 20 min, permeabilized with 0.5% Triton X-100 in PBS for 5 min, and blocked with 3% normal goat serum (Wako Pure Chemical Industries, Osaka, Japan) in PBS for 30 min. Anti-calnexin rabbit pAb (1:1000, Stress-

Gen), anti-PDI rabbit pAb (1:1000, StressGen), anti-syntaxin-6 rabbit mAb (1:100, CST), anti-ubiquitin mouse mAb (1:500, Millipore), anti-Nedd4-1 rabbit mAb (1:500, Abcam), and anti-CHMP2B rabbit pAb (1:500, Abcam) were used as primary antibodies and incubated for 18 h at 4  $^{\circ}$ C. Next, the cells were incubated with anti-mouse IgG Alexa Fluor 488 or 647 conjugates (1:2000, Invitrogen) for 1 h at room temperature. In some experiments, nuclei were counterstained by DRAQ7 (1:500, Biostatus, Leicestershire, UK). Fluorescent images were analyzed with the Olympus FV300 confocal laser scanning microscope system. All images were scanned by laser scanning microscope under identical conditions of  $512 \times 512$  pixels with a 12-bit/pixel resolution. Under each set of conditions, 10–20 cells in six randomly chosen fields were analyzed to evaluate the sizes of the Rab7 vesicles that contain aS using ImageJ software (National Institutes of Health). The diameter of each vesicle was determined by comparison with a standard, and the differences between the conditions were analyzed with the Mann-Whitney *U* test using GraphPad Prism. The data are expressed as the means  $\pm$  S.E.

**Immunohistochemistry**—Formalin-fixed, paraffin-embedded sections of the substantia nigra from five human patients with PD were subjected to immunohistochemical investigations using the avidin-biotin-peroxidase complex method with a Vectastain ABC kit (Vector Laboratories, Burlingame, CA). Polyclonal antibodies against Nedd4-1 (Sigma, 1:50; Millipore, 1:50) and Rab7A (Sigma, 1:50) were used as the primary antibodies. The sections were pretreated by heating for 15 min at 121  $^{\circ}$ C. Diaminobenzidine was used as the chromogen. The sections were counterstained with hematoxylin.

## RESULTS

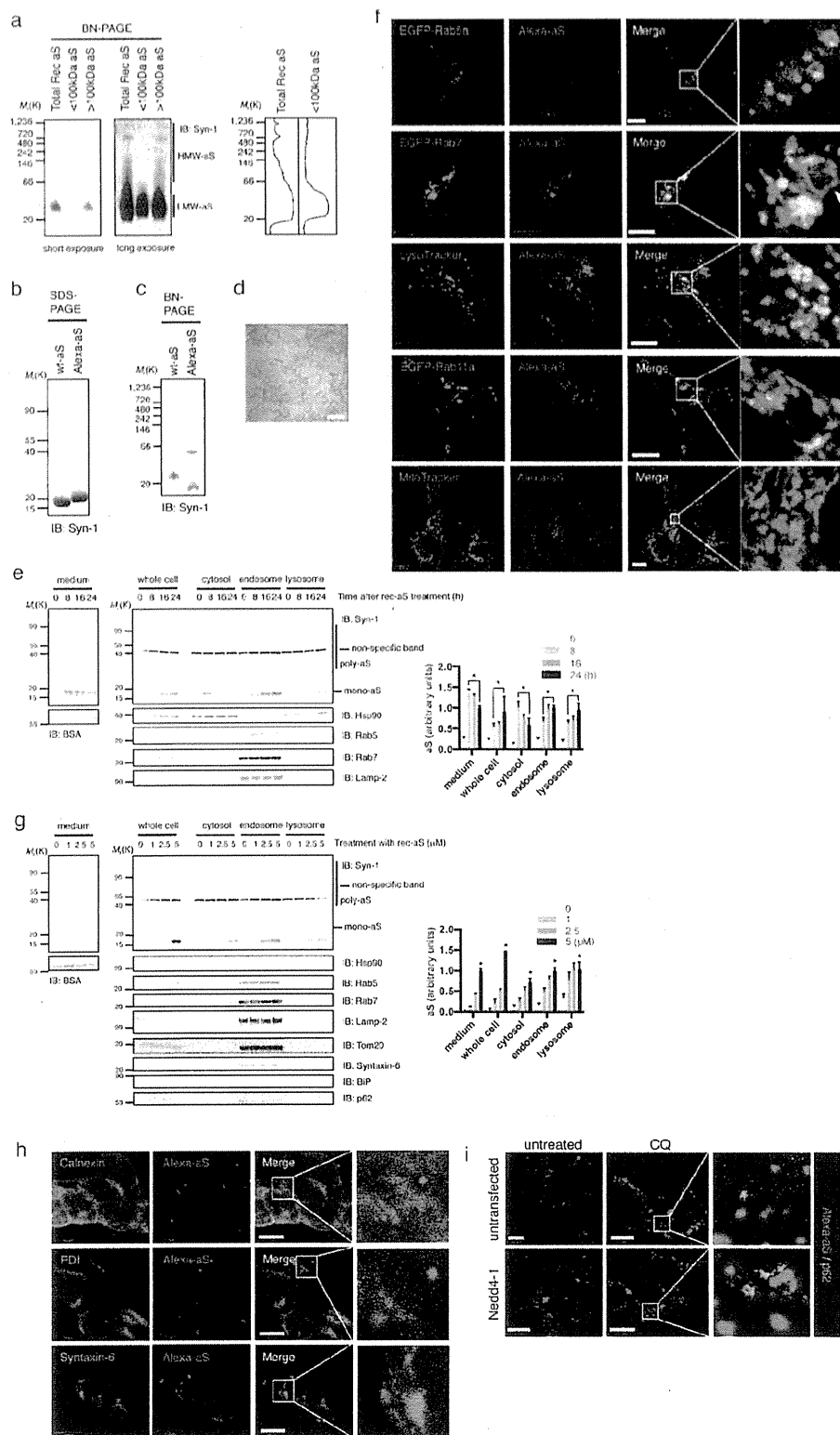
**aS Is Internalized and Accumulates in the Endosomes of Neuronal Cells**—First, we assessed the molecular weight of recombinant aS by BN-PAGE. The total recombinant aS migrated at  $\sim$ 40 kDa and showed two smaller peaks over 700 kDa (Fig. 1a). To eliminate the HMW aS species, recombinant aS was further separated using a 100-kDa pore-size filter, and LMW aS migrating at  $\sim$ 40 kDa was collected (designated as <100-kDa aS in Fig. 1a). To visualize the internalized aS, we prepared less than 100-kDa aS covalently bound to a fluorescent compound (Alexa-aS). The labeling efficiency was estimated to be  $\sim$ 2.29 (mol of dye)/(mol of protein) by fluorometric analysis (Alexa-aS in Fig. 1b). In BN-PAGE, Alexa-aS has two peaks, and the conformational changes might be caused during the process of fluorescence labeling or size exclusion chromatography (Fig. 1c). After treatment with 5  $\mu$ M Alexa-aS for 24 h, acceptable amounts of internalized aS were detected in SH-SY5Y cells (Fig. 1d). Subcellular fractionation analysis revealed that internalized aS appeared in the cytosol in the early phase (8 h) and thereafter gradually increased to 24 h. However, the increased aS in the endosomes and lysosomes was inversely proportional to the cytosolic aS, indicating the translocation of cytosolic aS to endo/lysosomal compartments (Fig. 1e). The kinetics of aS re-secretion into the medium was similar to that of the cytosolic aS. It should be noted that the endosomal fraction isolated by our method contains both early and late endosomes because this fraction is positive for Rab5 and Rab7 (Fig. 1e). Next, we



## Nedd4-1 Targets Internalized $\alpha$ -Synuclein to Endosomes

performed immunocytochemical analysis using SH-SY5Y cells expressing enhanced GFP-tagged Rab5a, Rab7, and Rab11a together with the acidic organelle marker LysoTracker or the mitochondrial marker MitoTracker. Most of the internalized

aS co-localized with Rab7-positive late endosomes and LysoTracker-positive structures and co-localized to a lesser degree with Rab5a-positive early endosomes and Rab11a-positive recycling endosomes. Note that none of the Alexa-aS corre-



sponds with the fluorescence of MitoTracker (Fig. 1f). Another intriguing finding is that large Alexa-aS inclusions were occasionally surrounded by Rab7-positive vesicular structures. The level of internalized aS was in proportion to the amount of aS added to the culture medium (Fig. 1g). We also observed re-secreted aS in the medium 1 h after replacing it with fresh medium. The endosomal fraction used in this study also contains mitochondria, Golgi, autophagosomes, and endoplasmic reticulum because this fraction was positive for mitochondrial Tom20, the Golgi marker, syntaxin-6, the autophagosome marker p62, and the endoplasmic reticulum marker BiP (Fig. 1g). To exclude the possibility that internalized aS was located in these organelles, SH-SY5Y cells treated with Alexa-aS were fixed and subjected to double immunostaining. As shown in Fig. 1h, none of the Alexa-aS-positive red dots were co-localized with endoplasmic reticulum proteins (calnexin and PDI) or syntaxin-6. In addition, we performed p62 immunostaining using the aS-exposed, Nedd4-1-expressing cells in the presence of the autophagy inhibitor CQ (Fig. 1i). The treatment with CQ caused numerous p62-positive fluorescent puncta, indicative of autophagosomes; however, the Alexa-aS-positive puncta were scarcely co-localized with p62.

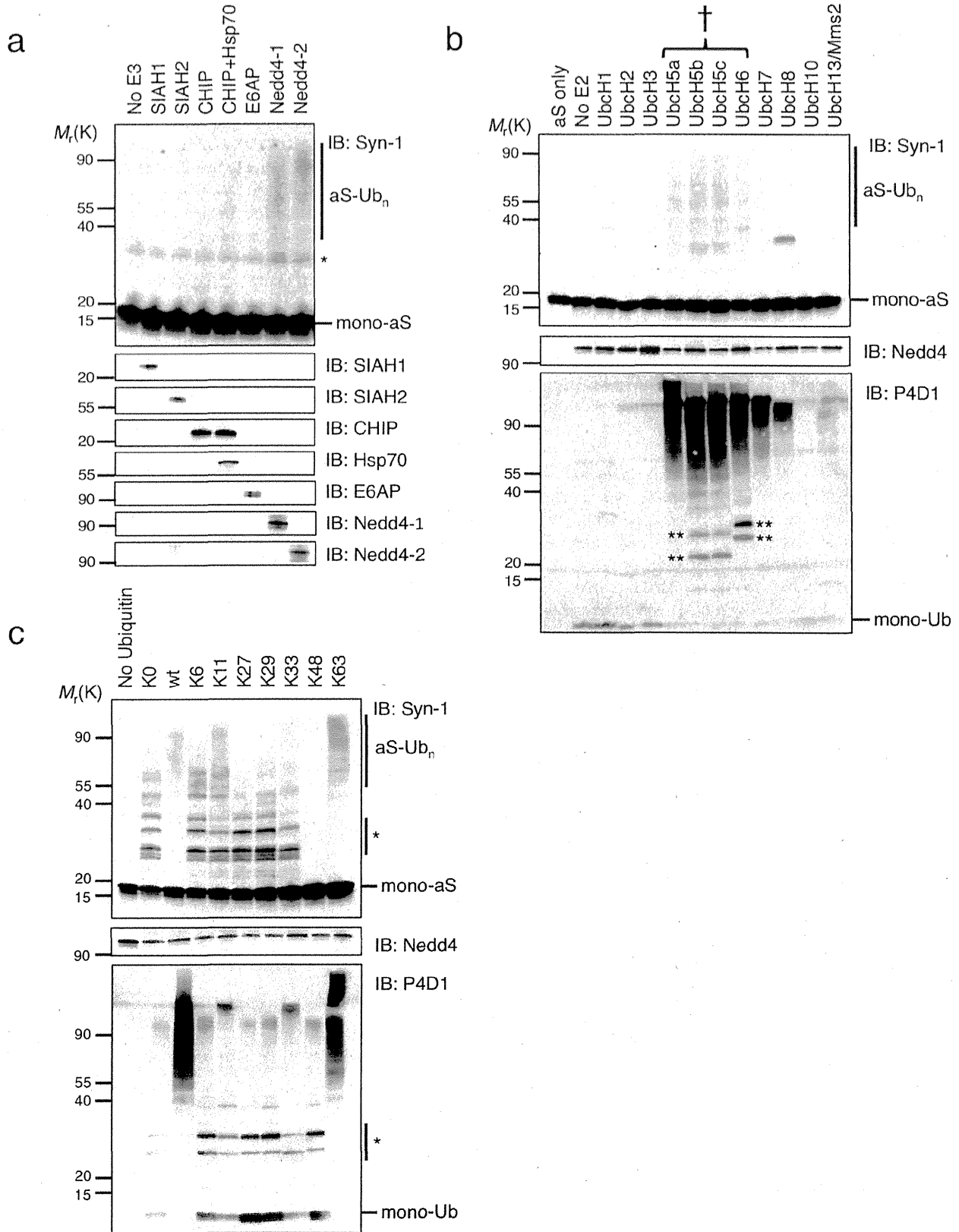
**Nedd4-1 Catalyzes the Lys-63- and Lys-11-linked Polyubiquitination of aS**—Several E3 ligases are known to catalyze the Lys-63-linked ubiquitination of aS, leading to its endolysosomal targeting and degradation (9, 17–20). To elucidate E3 ligase activity for aS, an *in vitro* aS ubiquitination assay was performed using the following human E3 ligases: SIAH-1, SIAH-2, Parkin, CHIP, Nedd4-1, and Nedd4-2 (Fig. 2a). In agreement with previous observations (9), we recapitulated that Nedd4-1 strongly catalyzed aS ubiquitination in the presence of UbcH5b. In addition, we found that the Nedd4-2 isoform equally ubiquitinates aS. The other E3 ligases failed to form ubiquitin chains on aS under the assay conditions employed. Nedd4-1 has been shown to prefer UbcH4, UbcH5b, UbcH5c, UbcH6, and UbcH7 as E2 ubiquitin-conjugating enzymes (21). To confirm this finding, aS ubiquitination by Nedd4-1 was re-evaluated with different E2 enzymes *in vitro*. We confirmed that UbcH5, UbcH6, UbcH7, and UbcH8 participated in the polyubiquitination by Nedd4-1 (Fig. 2b, lower panel). Among them, HMW aS-positive smears appeared solely in the samples containing UbcH5 and UbcH6 (Fig. 2b, upper panel). This finding is contradictory to a report by Tofaris *et al.* (9), which demonstrated that UbcH7 ubiquitinates aS together with Nedd4. This discrepancy could

be due to different experimental conditions. Ubiquitin has seven lysine residues (Lys-6, Lys-11, Lys-27, Lys-29, Lys-33, Lys-48, and Lys-63), all of which can form ubiquitin chains, resulting in various structures that alter the target protein in different ways. To determine the types of ubiquitin linkages preferentially generated by Nedd4-1, recombinant wild type aS, together with Nedd4-1, was incubated with ubiquitin with no active lysine residues (Lys-0) or ubiquitin with only one active lysine residue (Lys-6, Lys-11, Lys-27, Lys-29, Lys-33, Lys-48, and Lys-63). A polyubiquitination smear exclusively appeared when the samples were incubated with wild type and Lys-63 ubiquitin (Fig. 2c, lower panel). Polyubiquitinated aS species were detected in the presence of wild type, Lys-11-, Lys-63, and to a lesser extent Lys-33 ubiquitin, showing that Nedd4-1 preferentially promotes the assembly of the Lys-63-linked ubiquitin chain (Fig. 2c, upper panel).

**Lys-63 Linkage-specific Ubiquitination Enhances the Incorporation and Endosomal Targeting of Extracellular aS**—After crossing the plasma membrane, some of the internalized aS exits the membrane, and some remains in the cytoplasm for minutes. To confirm this possibility, we performed pulse-chase experiments to determine how long internalized aS remains in the cytosolic fraction. After exposure to 5  $\mu$ M recombinant aS for 24 h, the cells were extensively washed with PBS and further cultured for the indicated periods (0–60 min) in fresh medium in the absence of aS. The cytosolic fraction was isolated and subjected to Western blot analysis (Fig. 3a). After the removal of aS from the culture medium, the aS in the cytosolic fraction decreased by half within 5 min, demonstrating that the free cytosolic aS can easily cross the plasma membrane and immediately disappear from the cytosol. Based on these observations, it is tempting to speculate that specific ubiquitin modifications by Nedd4-1 might prevent aS secretion by leading to the juxtamembrane localization of aS to endosomal compartments. To confirm this possibility, we investigated whether Nedd4-1 silencing affects the re-secretion of internalized aS into the culture medium. As expected, after removing aS from the medium, Nedd4-1 silencing increased the aS re-secreted in the medium, whereas the elimination kinetics of cytosolic aS seem to be unaltered (Fig. 3, a and b). In addition to this re-secretion to the extracellular space, there are several possibilities that could explain the decrease of cytosolic aS as follows: proteolysis by the ubiquitin-proteasome system and

**FIGURE 1. Extracellular aS is readily internalized and accumulates in the endosomes of neuronal cells.** a, characterization of recombinant aS. On BN-polyacrylamide gels, a large peak around the molecular mass of 40 kDa, together with smears up to 200 kDa, are shown. Two small peaks over 700 kDa in recombinant aS were also detected (HMW-aS and Total Rec aS). After filtration with a 100-kDa pore size membrane, there is one peak at ~40 kDa (LMW-aS and <100-kDa aS). The results of densitometric analyses are shown in the right panel. b, immunoblot. b, on SDS-polyacrylamide gels, denatured recombinant aS appears in its monomeric form at 18 kDa. After labeling with Alexa Fluor, a slight electrophoretic mobility shift was observed. c, Alexa-labeled aS forms two bands on a BN-polyacrylamide gel. d, internalized aS was observed in SH-SY5Y cells treated with 5  $\mu$ M Alexa Fluor 488-aS for 24 h. Scale bar, 20  $\mu$ m. e, after treating SH-SY5Y cells with 5  $\mu$ M aS (below 100 kDa) for the indicated periods (0–24 h), internalized aS appeared in the cytosol in the early phase (8 h) and thereafter gradually decreased up to 24 h. Densitometry is shown in the right panel. The values for the amount of aS monomer in the medium, whole cell, cytosolic, endosomal, and lysosomal fractions were divided by the values of BSA, Hsp90, Hsp90, Rab7, or Lamp-2, respectively. Asterisk,  $p < 0.01$  by Dunnett's multiple comparisons test. f, images show live cells after treatment with 5  $\mu$ M Alexa Fluor 555-aS (Alexa-aS) for 24 h in the SH-SY5Y cells. Large (>2.5  $\mu$ m) Alexa-aS-positive inclusions are surrounded by EGFP-Rab7-positive structures (white arrowhead). Scale bar, 10  $\mu$ m. g, after treatment with recombinant aS, the level of internalized aS is in proportion to the amount of aS added to culture medium. One hour after changing with the fresh medium, re-secreted aS appears in the medium. Densitometry is shown in the right panel. Asterisk,  $p < 0.01$  by Dunnett's multiple comparisons test against 0, 1, or 2.5 ( $\mu$ M). h, after treatment with 5  $\mu$ M Alexa-aS for 24 h, SH-SY5Y cells were fixed and immunostained with organelle markers. The inset is a magnified picture of the square area. Scale bar, 10  $\mu$ m. i, SH-SY5Y cells without or overexpressing Nedd4-1 were pretreated by 5  $\mu$ M CQ for 2 h and further incubated in medium containing 5  $\mu$ M Alexa-conjugated aS for 24 h. The inset is a magnified picture of the square area. Scale bar, 10  $\mu$ m.

*Nedd4-1 Targets Internalized  $\alpha$ -Synuclein to Endosomes*



## Nedd4-1 Targets Internalized $\alpha$ -Synuclein to Endosomes

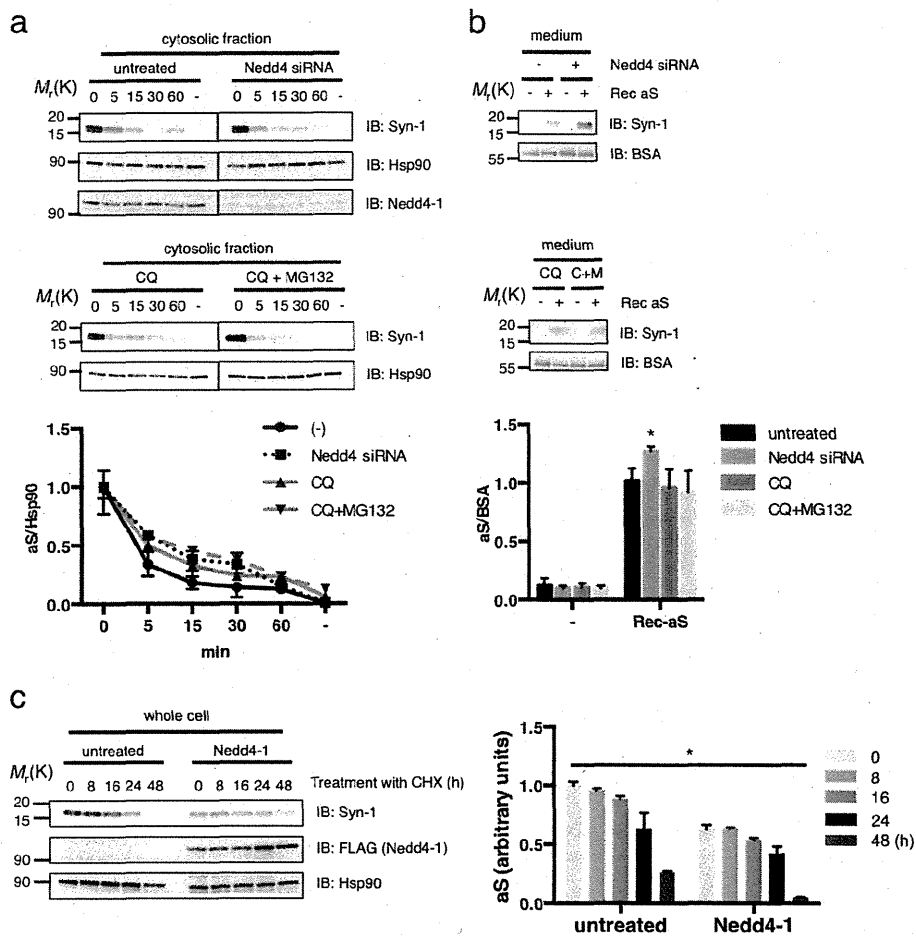


**FIGURE 3. Internalized aS is rapidly re-secreted to medium.** *a*, dynamic behavior of internalized aS was evaluated by pulse-chase experiments, using SH-SY5Y cells treated with 5  $\mu$ M aS for 24 h. After the removal of aS from the medium, the amount of aS in the cytosol decreased by half within 15 min. A similar result was obtained in Nedd4-1-silenced cells (*upper panel*). Note that the autophagy/lysosome inhibitor CQ and/or proteasome inhibitor MG132 pretreatment did not alter the kinetics of aS elimination from the cytosol (*middle panel*). The results of densitometric analyses are presented in the *lower panel*. Statistical analyses were performed by Dunnett's multiple comparisons test. *b*, immunoblot, *b*, to evaluate the aS re-secreted into the medium, the cells were incubated for 1 h with fresh medium after the aS exposure (5  $\mu$ M for 24 h). Note that aS was detected in the medium treated with recombinant aS (*Rec aS*). Silencing of Nedd4-1 substantially increased the level of re-secreted aS (*upper panel*). CQ and/or MG132 (*CQ and C+M*) treatments did not affect the aS re-secretion. The results of densitometric analyses are shown in the *lower panel*. Asterisk,  $p < 0.05$  by Dunnett's multiple comparisons test. *c*, Nedd4-1 expression affects the stability of endogenous aS. In the presence of the protein synthesis inhibitor cycloheximide (*CHX*), the basal amount of aS in cells overexpressing Nedd4-1 was significantly lower than that in the control cells (*asterisk*,  $p < 0.01$  by Sidak's multiple comparisons test). Densitometry from three independent experiments is presented (*right panel*).

sequestration to autophagic degradation. To investigate this, we examined the rate of aS disappearance in the presence of CQ and proteasomal inhibitors (MG132). Of note, treatment with CQ and/or MG132 did not affect the aS turnover up to 60 min (Fig. 3, *a* and *b*). These results suggest that most of the aS that disappeared from the cytosol is not removed by lysosomal and/or proteasomal degradation. To investigate the

effect of Nedd4-1 on the stability of extracellularly derived aS, we then investigated the time-dependent change of internalized aS in cells in the presence of the protein synthesis inhibitor cycloheximide. In the presence of 50  $\mu$ g/ml cycloheximide, the basal amount of endogenous aS in Nedd4-1-expressing cells was significantly lower compared with control cells, but the decay kinetics of intracellular aS seem to be

**FIGURE 2. Nedd4-1 catalyzes the Lys-63-linked polyubiquitination of aS.** *a*, *in vitro* ubiquitination assay of aS with recombinant E3 ligases. Both human Nedd4-1 and Nedd4-2 equally catalyzed aS polyubiquitination (*aS-Ub<sub>n</sub>*) in the presence of Ubch5b. Other E3 ligases failed to form ubiquitin chains on aS under the same conditions. Asterisk indicates the nonspecific bands. *b*, aS ubiquitination by Nedd4-1 was evaluated with various E2 enzymes *in vitro*. Western blotting using P4D1 antibody, which recognizes both mono- and polyubiquitin, shows an HMW smear in the samples incubated with Ubch5a, Ubch5b, Ubch5c, Ubch6, Ubch7, and Ubch8 (*lower panel*). Mono-ubiquitin (*Ub*) bands are weakly apparent in each lane. E2 enzymes with one or two ubiquitins were occasionally detected (*double asterisk*). Note that the HMW aS smear (*aS-Ub<sub>n</sub>*) visualized by anti-aS Ab (*Syn-1*) was solely detected in samples incubated with Ubch5a, Ubch5b, Ubch5c, and Ubch6. *c*, types of ubiquitin linkages preferentially generated by Nedd4-1. Recombinant wild type aS and Nedd4-1 were incubated together with ubiquitin that has no active lysine residue (*Lys-0*), or ubiquitin that has only one active lysine (*K*) residue (*Lys-6*, *Lys-11*, *Lys-27*, *Lys-29*, *Lys-33*, *Lys-48*, and *Lys-63*). Western blot using P4D1 antibody shows that the polyubiquitination smear is exclusively detected in the samples with wild type and *Lys-63* (*lower panel*). Polyubiquitinated, HMW aS species were detected in the samples incubated with wild type, *Lys-11*, *Lys-33*, and *Lys-63* ubiquitin (*upper panel*). Several bands at ~20–40 kDa are believed to be unspecific because these bands were also detected in the reaction with *Lys-0* ubiquitin (*asterisk*).

## Nedd4-1 Targets Internalized $\alpha$ -Synuclein to Endosomes

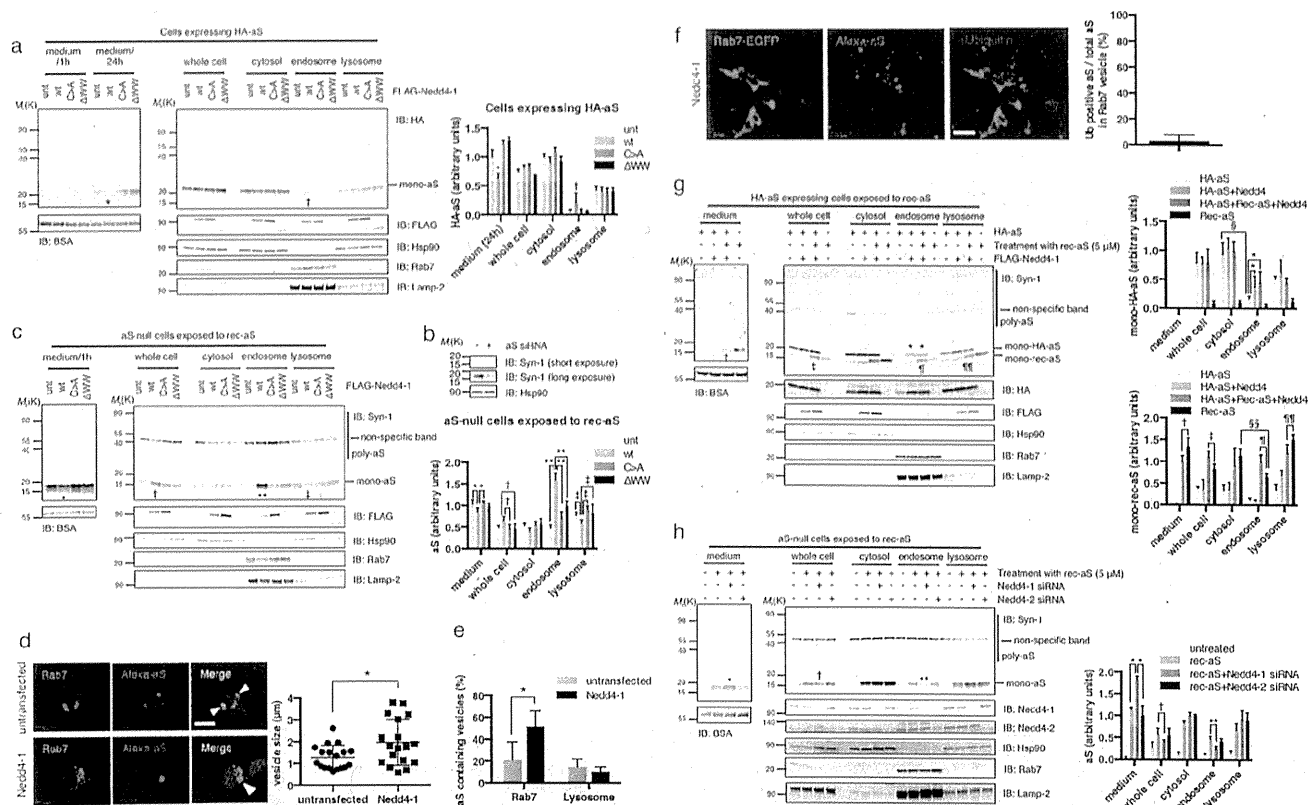


**FIGURE 4. Nedd4 facilitates the endosomal targeting of extracellularly derived and *de novo* synthesized aS.** *a*, Nedd4-1 facilitated the endosomal targeting of *de novo* synthesized aS in cultured cells. Wild type, C867A (C>A), or  $\Delta$ WW Nedd4-1 was co-transfected into SH-SY5Y cells stably expressing HA-tagged wild type-aS. Following 48 h of Nedd4-1 expression, the amount of aS significantly increased in the endosomal fraction (*dagger*,  $p < 0.05$ ) compared with the untransfected control (*unt*). Re-secreted aS levels decreased in the wild type Nedd4-1 overexpressing cells (*asterisk*,  $p < 0.01$ ). The densitometric value of HA-aS in the medium, whole cell, cytosolic, endosomal, and lysosomal fractions were divided by the values of BSA, Hsp90, Hsp90, Rab7, and Lamp-2, respectively (*right panel*). *IB*, immunoblot. *b*, endogenous aS level substantially declined after 48 h of aS silencing in SH-SY5Y cells. *c*, Nedd4-1 targeted the extracellularly derived aS to the endosomal compartment. After silencing endogenous aS, SH-SY5Y cells were further transfected with Nedd4-1 constructs for 24 h, which was followed by aS exposure ( $5 \mu\text{M}$  for 24 h). Compared with the results in HA-aS-expressing cells (Fig. 4*a*), extracellularly derived aS tended to accumulate in the endosomal compartments. Furthermore, the ectopic expression of wild type Nedd4-1 considerably increased the amount of endosomal aS (*double asterisk*,  $p < 0.01$ ). In contrast, the amount of aS in the medium and the lysosomal fraction slightly, but significantly, decreased in wild type Nedd4-1-expressing cells (*asterisk* and *double dagger*, respectively,  $p < 0.05$ ). The densitometric values of monomeric aS in each fraction are presented in the *right panel*. *d*, Nedd4-1 expression significantly increased the size of aS-positive inclusions surrounded by Rab7-positive endosomal structures (*white arrows*) in SH-SY5Y cells exposed to Alexa-aS. *Scale bar*,  $10 \mu\text{m}$ . *Asterisk*,  $p < 0.05$  by two-tailed Mann-Whitney *U* test (*right panel*). *e*, number of Rab7-positive or LysoTracker-positive vesicles having Alexa-aS was quantitatively analyzed. *Asterisk*,  $p < 0.01$  Sidak's multiple comparisons test. *f*, cells overexpressing Rab7-EGFP and Nedd4-1 were treated with Alexa-aS and then subjected to immunostaining. *Scale bar*,  $10 \mu\text{m}$ . *g*, *de novo* synthesized HA-aS in the endosome was 20% versus the cytosolic aS (5) cells exposed to Alexa-aS. *Asterisk*,  $p < 0.05$  by Dunnett's multiple comparisons test). The densitometric values of mono-aS are shown in the *right panel*. In these cells, the level of endosomal aS was decreased (*double asterisk*,  $p < 0.05$ ), whereas re-secreted aS was significantly increased (*asterisk*,  $p < 0.001$ ). The densitometric values of monomeric aS in each fraction is presented in the *right panel*.

unchanged between control and Nedd4-1-expressing cells (Fig. 3*c*). We observed that Nedd4-1 did not influence the turnover of *de novo* synthesized HA-aS (data not shown).

**Nedd4-1 Facilitates the Endosomal Targeting of aS**—Intracellular aS is divided into two types based on its derivation as follows: aS internalized from the extracellular space and as *de novo* synthesized aS. Thus, the intracellular aS of different origins may have distinct fates during the process of intracellular vesicular transport. To determine whether Nedd4-1 specifies the intracellular trafficking of aS of different origins, we co-expressed wild type, C867A, or  $\Delta$ WW Nedd4-1 in SH-SY5Y cells stably expressing HA-tagged aS. Following 48 h of Nedd4-1 expression, the amount of aS increased in the endosomal fraction (Fig. 4*a*). This finding is consistent with earlier research showing that Nedd4-1 promotes the endolysosomal sorting of

aS for degradation (9). After washing off the medium, we did not detect re-secreted aS within 1 h, but a detectable amount of extracellular aS was observed up to 24 h (Fig. 4*a*). In an inverse correlation with endosomal aS, the level of re-secreted aS was slightly increased in wild type Nedd4-1-overexpressing cells. To monitor the trafficking of extracellular aS in more detail, endogenous aS of SH-SY5Y cells was silenced prior to rec-aS exposure (Fig. 4, *b* and *c*). Compared with the results using HA-aS expressing cells, extracellularly derived aS tended to accumulate in the endosomal compartments (Fig. 4*c*). Furthermore, the ectopic expression of wild type Nedd4-1 substantially augmented the endosomal sorting of internalized aS. In contrast to the up-regulation of endosomal aS, we found that aS levels in the lysosomal fraction decreased slightly in Nedd4-1-expressing cells. The excessive amount of Nedd4-1 may have

## Nedd4-1 Targets Internalized $\alpha$ -Synuclein to Endosomes

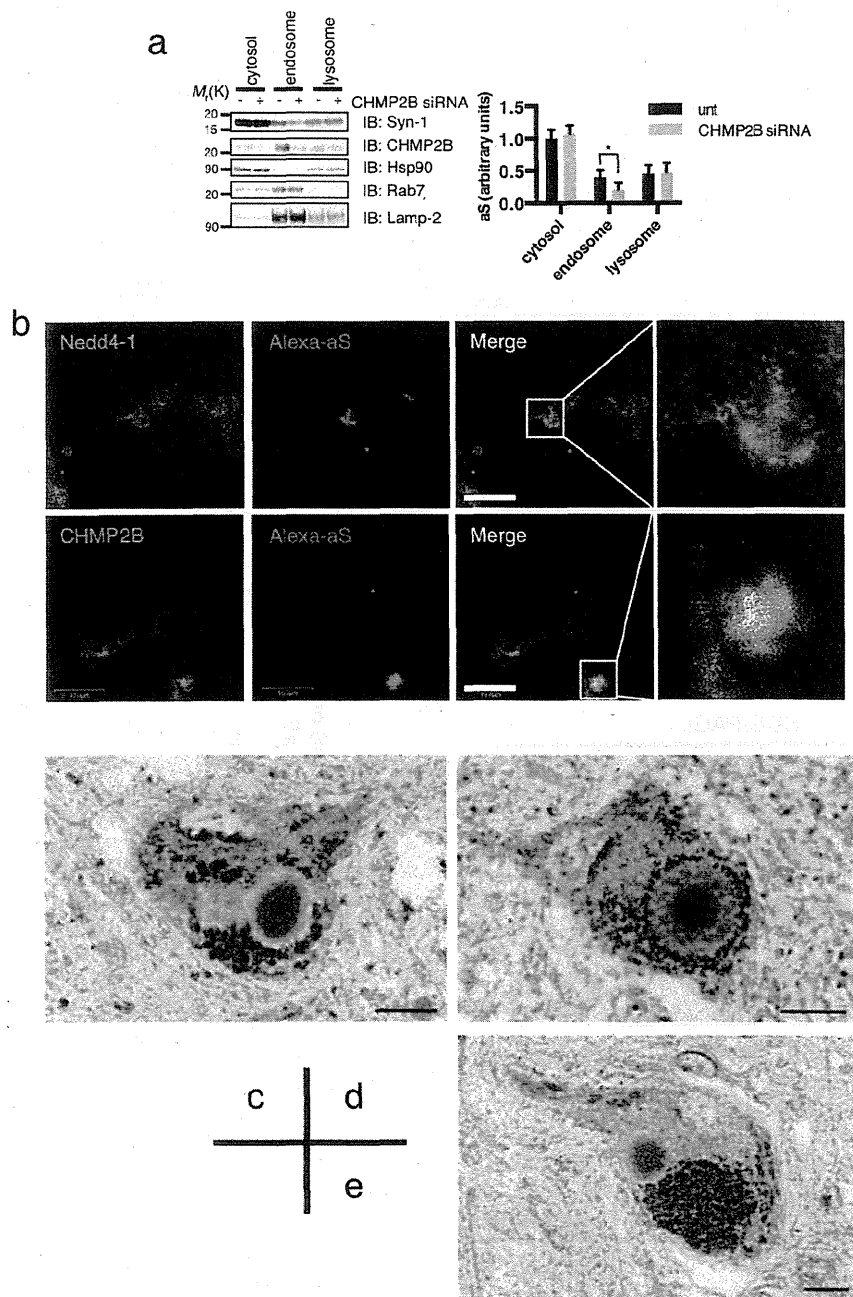


**FIGURE 5. Nedd4-1 accumulated to both *in vitro* and *in vivo* aggregate formations.** *a*, silencing of CHMP2B markedly reduced the amount of recombinant aS in the endosomes (asterisk,  $p < 0.01$ ). The densitometric values of monomeric aS in each fraction are presented in the *right panel*. *IB*, immunoblot. *b*, immunocytochemical analyses of aS inclusions *in vitro*. Nedd4-1-expressing SH-SY5Y cells were treated with 5  $\mu$ M Alexa-aS for 24 h and then subjected to immunostaining. aS-positive dense signal over 3  $\mu$ m diameter was defined as an inclusion. Note that aS-positive inclusions were partly co-localized with Nedd4-1 and CHMP2B. *Scale bar*, 10  $\mu$ m. *c–e*, immunohistochemical analysis of substantia nigra from postmortem PD brain. The core structure of Lewy bodies showed immunoreactivity with Rab7A (*c*), and Nedd4-1 (*d*, Millipore; *e*, Sigma). *Scale bar*, 10  $\mu$ m.

hampered extracellularly derived aS transport from the endosome to the lysosome because Nedd4-1 expression significantly increased both the occurrence and size of aS-positive inclusions surrounded by Rab7-positive endosomal structures (Fig. 4, *d* and *e*). Theoretically, the cargo's ubiquitin modification needs to be detached before entry into the endosomal luminal space (22). Thus, it is feasible that only 3% of Alexa-labeled recombinant aS in Rab7-positive vesicles was ubiquitinated in this cel-

lular model (Fig. 4*f*). The importance of ubiquitin-dependent sorting machinery is strengthened by the fact that the silencing of CHMP2B, a component of the endosomal sorting complex required for transport (ESCRT), resulted in a marked reduction of endosomal targeting of recombinant aS (Fig. 5*a*). As far as the subcellular distribution is concerned, *de novo* synthesized HA-aS in the endosome was 20% *versus* the cytosolic aS. By contrast, the internalized recombinant aS was more extensively

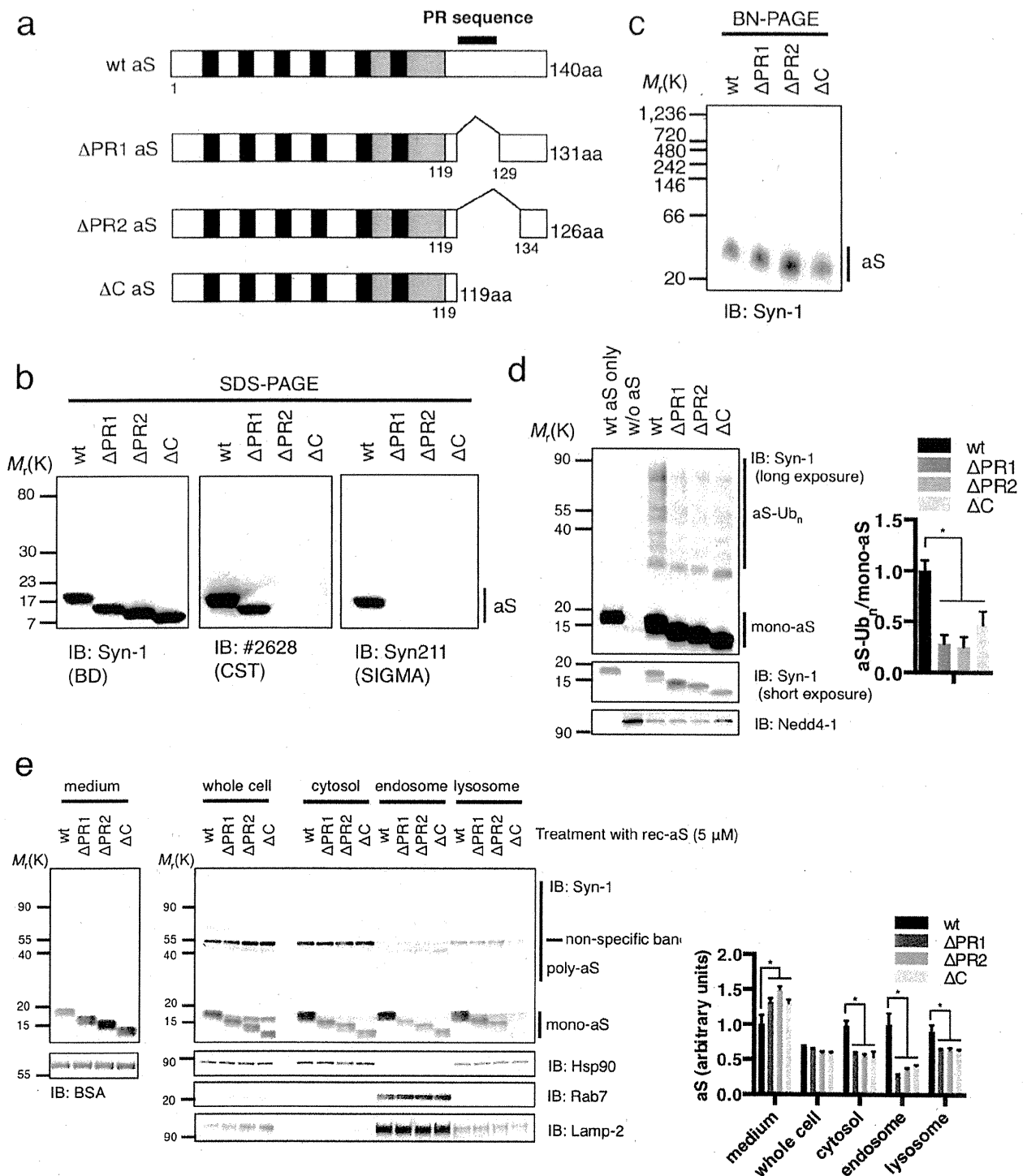


## Nedd4-1 Targets Internalized $\alpha$ -Synuclein to Endosomes

distributed in the endosome (50% compared with the cytosolic aS) (Fig. 4g). To further establish the role of Nedd4 in the endosomal targeting of aS, we knocked down endogenous Nedd4-1 or Nedd4-2 prior to aS exposure. As shown in Fig. 4h, a substantial decrease of endosomal aS and an elevation of extracellular aS were observed in Nedd4-1-deficient cells, although this effect was unremarkable in Nedd4-2-silenced cells. This find-

ing may indicate that Nedd4-1 and Nedd4-2 are functionally distinct and that Nedd4-1 is the main human Nedd4 isoform that affects the fate of internalized aS in human neuronal cells.

*Nedd4-1 Is a Component of aS-positive Inclusions in Cellular Model and the Brain Lesion of PD*—To verify the functional role of Nedd4-1 in the formation of aS-positive inclusions, SH-SY5Y cells transfected with Nedd4-1 were treated with Alexa-aS for



## Nedd4-1 Targets Internalized $\alpha$ -Synuclein to Endosomes

24 h and then subjected to double immunostaining. As shown in Fig. 5*b*,  $\alpha$ S-positive inclusions were partly positive for Nedd4-1 and a component of ESCRT machinery, CHMP2B. This outcome indicates that the ESCRT pathway is closely involved in the process of  $\alpha$ S inclusion formation. Furthermore, we found that the core structure of LBs, a pathological hallmark of PD, showed strong immunoreactivity with Rab7A (Fig. 5*c*) and Nedd4-1 (Fig. 5, *d* and *e*).

**C-terminal Residues of  $\alpha$ S Are Required for Nedd4-1-mediated Endosomal Targeting**—Nedd4-1 recognizes PR regions of target proteins via the WW domain, thereby exerting its E3 ligase activity. Although  $\alpha$ S does not have a canonical PPXY motif, it contains a relatively proline-rich domain (PVDPDNEAYEMPSEEGYQDYEP EA) at its C terminus (9). To determine the functional importance of the PR sequence in Nedd4-1-mediated ubiquitination, three deletion mutants of  $\alpha$ S, designated  $\Delta$ PR1(1–119 and 129–140),  $\Delta$ PR2(1–119 and 134–140), and  $\Delta$ C(1–119), were generated and expressed in *E. coli* (Fig. 6, *a* and *b*). To discriminate among these mutants by Western blotting, the following Abs were used: Syn-1, Syn211, and 2628. The Syn-1 Ab, which recognizes aa 91–99, detected all mutant proteins, whereas the Syn211 Ab, which recognizes aa 121–125, did not detect all mutant proteins. The 2628 antibody, the exact specificity of which is unknown, detected wild type and  $\Delta$ PR1  $\alpha$ S but not  $\Delta$ PR2 and  $\Delta$ C  $\alpha$ S (Fig. 6*b*). Not only wild type  $\alpha$ S but also mutant  $\alpha$ S migrated to  $\sim$ 30–40 kDa (Fig. 6*c*). After the *in vitro* ubiquitination assay, all recombinant proteins were subjected to Western blotting using the Syn-1 Ab. We found that wild type  $\alpha$ S produced high molecular weight bands in the presence of UbcH5b. In contrast, high molecular weight bands appeared less noticeable in samples containing these mutants (Fig. 6*d*). These results provide evidence that the PR sequence is required for  $\alpha$ S ubiquitination by Nedd4-1. To further substantiate and extend these observations, SH-SY5Y cells were exposed to 5  $\mu$ M wild type  $\alpha$ S or to mutant  $\alpha$ S lacking the PR sequence for 24 h. Intriguingly, we found that the endolysosomal as well as the cytosolic targeting of all mutants was greatly inhibited compared with that of wild type  $\alpha$ S, whereas the PR mutation substantially increased the amount of re-secreted  $\alpha$ S in the culture media (Fig. 6*e*). These results suggest that mutant  $\alpha$ S forms that show disturbance in Nedd4-mediated polyubiquitination cannot be sorted into endolysosomal compartments. Furthermore, at least the nine amino acids (PR sequence  $^{120}$ PDNEAYEMP $^{128}$ ) in the C terminus of  $\alpha$ S may be required for endosomal targeting of  $\alpha$ S by Nedd4-1.

**Pro-120 and Pro-128 in the PR Sequence Are Essential for Nedd4-1-mediated Endosomal Targeting of  $\alpha$ S**—To further elucidate which proline residue(s) within the PR sequence are

essential for the Nedd4-1-mediated  $\alpha$ S ubiquitination, we generated recombinant  $\alpha$ S in which proline 120 or proline 128 was replaced with alanine (P120A and P128A, respectively, in Fig. 7, *a* and *b*). Because HECT-type ubiquitin ligase sometimes attaches to phosphorylated serine/threonine residues (23), serine 129 (Ser-129), which is a major phosphorylation site in  $\alpha$ S, was also substituted with alanine (S129A, in Fig. 7, *a* and *b*). After size exclusion filtration using a 100-kDa Amicon filter, all mutant  $\alpha$ S and wild type  $\alpha$ S migrated to  $\sim$ 40 kDa on BN-PAGE (Fig. 7*c*). *In vitro* ubiquitination assays using the UbcH5b E2 enzyme revealed that P120A and P128A  $\alpha$ S mutants were less prone to being polyubiquitinated by Nedd4-1 compared with wild type  $\alpha$ S, whereas the ubiquitination of S129A  $\alpha$ S by Nedd4-1 was comparable with that of wild type- $\alpha$ S (Fig. 7*d*), suggesting that Pro-120 and Pro-128 are key residues for the Nedd4-1-mediated ubiquitination of  $\alpha$ S. Intriguingly, we found that the level of intracellular  $\alpha$ S was slightly decreased in P120A mutant  $\alpha$ S, whereas P120A substitution substantially increased the amount of re-secreted  $\alpha$ S in the culture media (Fig. 7*e*). Furthermore, subcellular fractionation analysis showed that the cytosolic and endosomal targeting of P120A and P128A mutants was disturbed compared with wild type and S129A  $\alpha$ S. Cumulatively, these findings confirm the functional importance of the Pro-120 and Pro-128 residues for Nedd4-1-mediated endosomal targeting of  $\alpha$ S.

## DISCUSSION

One of the most exciting themes emerging from recent neurodegenerative research is the transcellular spread of pathogenic protein aggregates in affected brain lesions. To understand how aggregated proteins, such as  $\alpha$ S, travel from cell to cell, the underlying mechanism responsible for the uptake and secretion of aggregate-prone proteins must be elucidated. The internalization of  $\alpha$ S by cells is thought to be initiated by  $\alpha$ S attachment to the outer leaflet of the plasma membrane via its amphipathic N-terminal domain (24, 25), which induces membrane curvature, tubulation, and breaking (26). Prior evidence has suggested that endocytic processes play a role in  $\alpha$ S internalization in both neuronal and glial cells (3, 4, 27); however,  $\alpha$ S internalization was not found to be completely blocked by the disruption of the endocytic machinery. These findings indicate that mechanisms other than endocytosis may contribute to  $\alpha$ S internalization (3, 4, 27). Indeed, there is evidence showing that fibrillar and nonfibrillar oligomeric  $\alpha$ S species are incorporated via the endocytic machinery and that monomeric  $\alpha$ S directly passes through the plasma membrane (4). Unfortunately, how  $\alpha$ S crosses the plasma membrane remains to be determined.

**FIGURE 6. C-terminal residues of  $\alpha$ S are required for  $\alpha$ S endosomal targeting mediated by Nedd4-1.** *a*,  $\alpha$ S contains a relatively PR sequence at its C terminus ( $^{120}$ PDNEAYEMPSEEGYQDYEP EA $^{140}$ ). Three deletion mutants of  $\alpha$ S, designated  $\Delta$ PR1(1–119 and 129–140),  $\Delta$ PR2(1–119 and 134–140), and  $\Delta$ C(1–119), were generated to determine the functional importance of the PR motif in Nedd4-1-mediated ubiquitination. *b*, characterization of the  $\alpha$ S deletion mutants by SDS-PAGE. Syn-1 antibody, which recognizes amino acids (aa) 91–99, detected all mutant proteins, whereas Syn211 antibody, which recognizes aa 121–125, did not detect all mutant proteins. The 2628 antibody, the exact specificity of which is unknown, detected wild type and  $\Delta$ PR1  $\alpha$ S, but not  $\Delta$ PR2 and  $\Delta$ C  $\alpha$ S. *c*, characterization of the  $\alpha$ S deletion mutants by BN-PAGE. Both wild type  $\alpha$ S and mutant  $\alpha$ S migrated to  $\sim$ 30–40 kDa. *d*, *in vitro* ubiquitination assays using UbcH5b reveal that all of the PR mutants had a reduced ability to form Nedd4-1-mediated polyubiquitinated  $\alpha$ S ( $\alpha$ S- $Ub_n$ ). The densitometric values of  $\alpha$ S- $Ub_n$  smear on long exposure image were normalized by the values of mono- $\alpha$ S on short exposure images ( $p < 0.01$ ; each mutant is compared with wild type by Dunnett's multiple comparisons test). *e*, SH-SY5Y cells were exposed to 5  $\mu$ M wild type and mutant  $\alpha$ S lacking the PR sequence for 24 h and subjected to Western blot analysis. Note that the endolysosomal as well as the cytosolic targeting of all of the PR mutants was greatly inhibited compared with that of wild type  $\alpha$ S, whereas the PR mutation substantially increased the amount of re-secreted  $\alpha$ S in the medium (asterisk,  $p < 0.01$ ; each mutant is compared with wild type by Dunnett's multiple comparisons test). The right panel shows the amount of monomeric  $\alpha$ S normalized by each fraction marker. *IB*, immunoblot.

## Nedd4-1 Targets Internalized $\alpha$ -Synuclein to Endosomes

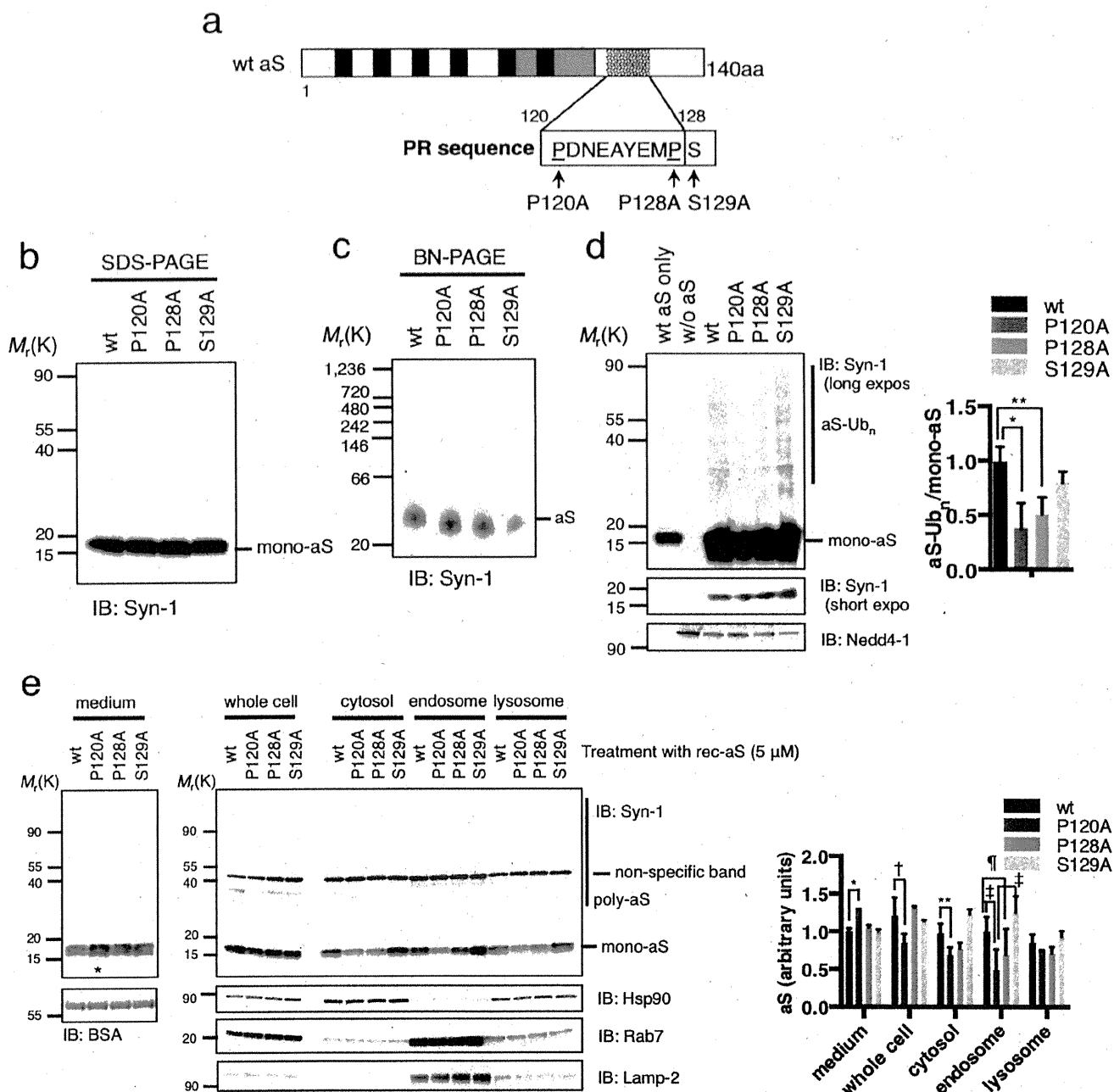


**FIGURE 7. Pro-120 might be a core frame of the aS PR sequence for Nedd4-1-mediated aS endosomal targeting.** *a*, schematic presentation of PR sequence ( $^{120}$ PDNEAYEMP $^{128}$ ) in human aS. The PR sequence contains two proline residues (Pro-120 and Pro-128), and Ser-129 flanks the PR sequence. *b*, characterization of the aS proline-substituted mutants by SDS-PAGE. All mutants appear as monomeric aS (15–20 kDa) under denaturing conditions. *c*, mutants and wild type aS (after 100-kDa size exclusion) showed LMW aS by BN-PAGE. *d*, *in vitro* ubiquitination assays using UbCH5b reveal that P120A and P128A aS mutants were less prone to polyubiquitination (aS-Ub<sub>n</sub>) by Nedd4-1 compared with wild type aS, whereas the ubiquitination of S129A aS by Nedd4-1 was comparable with that of wild type aS. The values for the amount of aS-Ub<sub>n</sub> from long exposure are divided by the values of mono-aS from short exposure (asterisk,  $p < 0.01$ ; double asterisk,  $p < 0.05$  by Dunnett's multiple comparisons test). *e*, 5H-SY5Y cells were exposed to 5  $\mu$ M wild type aS or mutant, proline-substituted aS for 24 h and subjected to Western blot analysis. The levels of intracellular and cytosolic aS were slightly decreased in the P120A mutant aS (dagger,  $p < 0.001$ ; double asterisk,  $p < 0.05$ ), although this mutant substantially increased the amount of re-secreted aS in the culture media (asterisk,  $p < 0.05$ ). Note that the cytosolic and endosomal targeting of P120A and P128A mutants was disturbed compared with wild type and S129A aS (double dagger,  $p < 0.01$ ; pilcrow,  $p < 0.05$  by Dunnett's multiple comparisons test). The right panel shows the amount of monomeric aS normalized by each fraction marker. IB, immunoblot.

Several possibilities have been postulated, including direct penetration (25), the formation of annular pore-like structures (28), and macropinocytosis (5, 29). Although this notion is provocative, it is supported by analogous studies in other neurodegen-

erative diseases, such as polyglutamine disease, in which polyQ aggregates can rapidly enter the cytosolic compartment of mammalian cells and nucleate the aggregation of soluble proteins with these polyQ tracts (30). Regardless of the mecha-

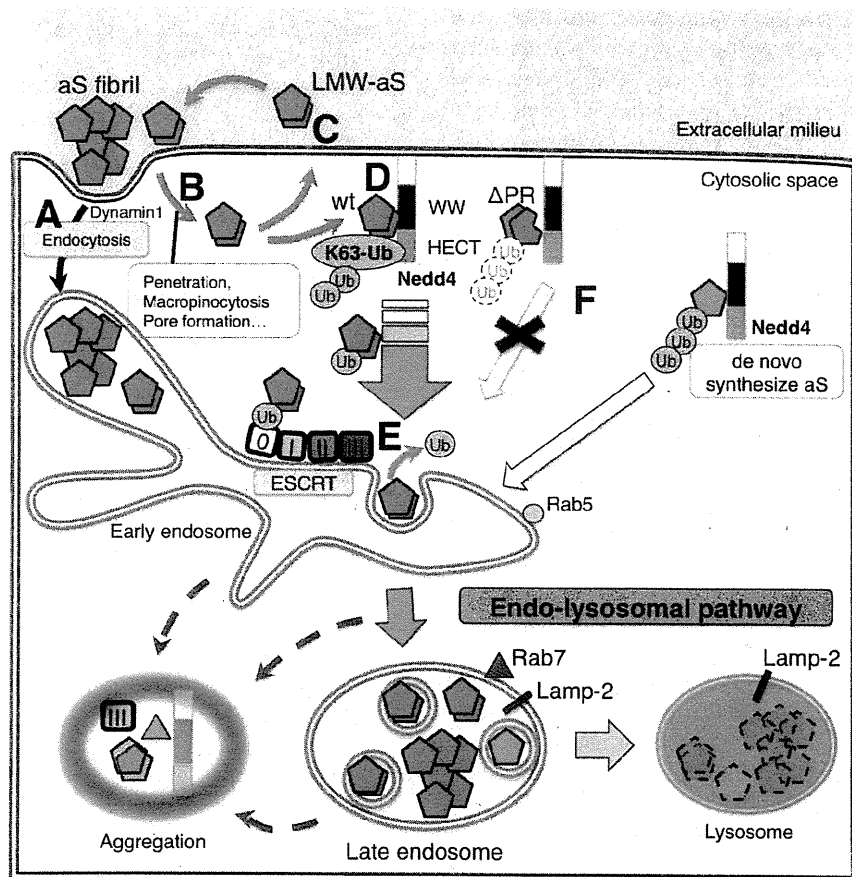


FIGURE 8. **Nedd4-1 determines the fate of internalized aS in neuronal cells.** Some extracellular aS is incorporated into neuronal cells by a dynamin-dependent mechanism and is transported into early endosomes (A). In contrast, a substantial amount of aS directly enters the cytosolic space, presumably via penetration of the plasma membrane (B). After crossing the plasma membrane, some of the internalized aS will exit the cells (C) and some will remain in the cytosol for minutes. Plasma membrane-resident Nedd4-1 binds to the C terminus of internalized aS through the WW domain and attaches a Lys-63-linked polyubiquitin chain to aS, thereby facilitating endosomal targeting (D). Most likely, the ESCRT complex recognizes the Lys-63-ubiquitinated aS and transports the aS into the late endosome through invagination of the endosomal membrane (E), which may promote aS degradation in lysosomes. The aS mutant that lacked the PR motif failed to sort into the late endosomes, most likely because it cannot be recognized by Nedd4-1 (F).

nisms involved in aS internalization, some extrinsic aS species can likely enter neuronal and/or glial cells directly, where they gain access to the cytosolic compartment and are subjected to further processing, modification, and transport.

In this study, we found that Nedd4-linked Lys-63 ubiquitination specified the fate of extrinsic and *de novo* synthesized aS by facilitating aS targeting to endosomal compartments. It appears that immediately after passing through the plasma membrane, the majority of the internalized aS is located just beneath the plasma membrane. Because Nedd4 localizes to the cytosolic space by associating with the inner plasma membrane leaflet via its C2 domain, Nedd4-1 likely preferentially catalyzes juxtamembrane aS localization. This notion is supported by previous studies showing that Nedd4-1-mediated ubiquitination is closely linked to the turnover and trafficking of cell-surface receptors (31, 32). Although aS does not contain the canonical PPXY motif known to interact with the WW domain of Nedd4-1, the WW domain can recognize several motifs other than PPXY with varying affinities (33). For example, the WW domains of Nedd4 families recognize PPLP, PR motifs, and phospho-(Ser/Thr) residues, as well as PPXY (23). Our obser-

vation using deletion mutants provides evidence that the PR sequences in the C terminus of aS, particularly residues Pro-120 and Pro-128, are important for proper recognition by Nedd4-1. It is uncertain why Nedd4 silencing did not show a similar effect on the cytosolic aS accumulation as the  $\Delta$ PR and P120A mutations. However, this could be attributed to the insufficient silencing efficacy of Nedd4 in cultured cells. The fact that a major phosphorylation site, Ser-129, occurs in the region flanking the aS PR sequence (34, 35) raises the possibility that phosphorylation at Ser-129 might affect Nedd4-1-mediated ubiquitination. However, this effect is not likely, as we found no difference in aS ubiquitination regardless of the presence of Ser-129.

Nedd4-1 catalyzes both the mono-ubiquitination and Lys-63-linked polyubiquitination of target proteins (36). Lys-63-linked ubiquitination is implicated in various cellular activities, including protein trafficking, DNA repair, stress responses, and signal transduction (37). Although mono-ubiquitination appears to be involved in endocytic trafficking, additional Lys-63-linked polyubiquitination is known to accelerate this trafficking process (38). More specifically, Lys-63-linked polyubi-

## Nedd4-1 Targets Internalized $\alpha$ -Synuclein to Endosomes

ubiquitination serves as a signal for protein sorting into the ESCRT-driven multivesicular body pathway by inward membrane invagination of endosomes (39). Previous studies have shown that LB showed immunoreactivity against ESCRT components such as CHMP2B and VPS4 (2, 40, 41). These findings are interesting when considering the biogenesis of LB because the pale body, a possible precursor of LB, often contains lysosomes, vacuolar structures, and ubiquitinated proteins (42). Moreover, our observation that Nedd4-1 is a component of LB also strengthens the hypothesis that the Nedd4-regulated endo/lysosomal sorting machinery might be involved in the buildup of aS-positive aggregates in affected brain lesions.

The mechanism by which cytosolic aS moves into the endosomal vesicle is poorly understood; however, our result showing that the silencing of CHMP2B, a component of ESCRT-III, can disrupt the endosomal accumulation of aS indicates the functional relevance of ESCRT machinery in the endolysosomal targeting of aS. Mechanistically, the endosomal targeting of ubiquitinated cargo and the formation of multivesicular bodies are mediated by the upstream ESCRT complexes (ESCRT-0, -I, and -II) on the surface of the endosomal membrane. ESCRT-III then recruits de-ubiquitinating enzymes to remove ubiquitin from the cargo before incorporating them into the intraluminal vesicles of multivesicular bodies (43, 44). This could be a reason why we failed to detect strong ubiquitination in aS-positive inclusions surrounded by Rab7-positive late endosomes. Another important finding of this study is that the Nedd4-1-mediated endosomal targeting of aS was accompanied by a prominent enlargement of the late endosome. Intriguingly, a marked enlargement of endosomal vesicles has also been shown in the affected brain and in a cellular model of Alzheimer disease (45, 46). Why the overexpression of Nedd4-1 down-regulated the lysosomal accumulation of aS in this study is uncertain. One possible explanation is that the excessive accumulation of aS might prevent early-to-late endosome transition. Indeed, previous studies have shown that aS itself is closely involved in vesicular trafficking events, such as Rab-mediated endoplasmic reticulum-Golgi transport and endosomal trafficking (47–49). An alternative possibility is that aS aggregates may decrease the lysosomal burden by inducing lysosomal rupture (50).

In summary, we found that Nedd4-1 markedly facilitated aS internalization, which was linked to Lys-63 linkage-specific polyubiquitination. Our results demonstrate how Lys-63-linked ubiquitination contributes to the endosomal targeting and the endosomal accumulation of aS and therefore may be involved in the propagation and formation/clearance of Lewy pathology in PD (Fig. 8). Although the concept of the cell-to-cell transmission of aberrant proteins has been recognized as a common phenomenon in many neurodegenerative diseases, the molecular mechanisms underlying the spread of protein misfolding likely differ depending on the biochemical nature of the protein aggregate, the level of cellular stress, and the cell type. Further studies are needed to gain insight into the cellular mechanisms of disease progression and to identify molecular targets for therapeutic intervention in PD and other neurodegenerative diseases.

*Acknowledgment*—We are grateful to Nanae Osanai for excellent technical assistance.

### REFERENCES

1. Angot, E., Steiner, J. A., Hansen, C., Li, J. Y., and Brundin, P. (2010) Are synucleinopathies prion-like disorders? *Lancet Neurol.* **9**, 1128–1138
2. Hasegawa, T., Konno, M., Baba, T., Sugeno, N., Kikuchi, A., Kobayashi, M., Miura, E., Tanaka, N., Tamai, K., Furukawa, K., Arai, H., Mori, F., Wakabayashi, K., Aoki, M., Itoyama, Y., and Takeda, A. (2011) The AAA-ATPase VPS4 regulates extracellular secretion and lysosomal targeting of  $\alpha$ -synuclein. *PLoS One* **6**, e29460
3. Konno, M., Hasegawa, T., Baba, T., Miura, E., Sugeno, N., Kikuchi, A., Fiesel, F. C., Sasaki, T., Aoki, M., Itoyama, Y., and Takeda, A. (2012) Suppression of dynamin GTPase decreases  $\alpha$ -synuclein uptake by neuronal and oligodendroglial cells: a potent therapeutic target for synucleinopathy. *Mol. Neurodegener.* **7**, 38
4. Lee, H. J., Suk, J. E., Bae, E. J., Lee, J. H., Paik, S. R., and Lee, S. J. (2008) Assembly-dependent endocytosis and clearance of extracellular  $\alpha$ -synuclein. *Int. J. Biochem. Cell Biol.* **40**, 1835–1849
5. Lee, S. J., Desplats, P., Sigurdson, C., Tsigelny, I., and Masliah, E. (2010) Cell-to-cell transmission of non-prion protein aggregates. *Nat. Rev. Neurol.* **6**, 702–706
6. Hasegawa, M., Fujiwara, H., Nonaka, T., Wakabayashi, K., Takahashi, H., Lee, V. M., Trojanowski, J. Q., Mann, D., and Iwatsubo, T. (2002) Phosphorylated  $\alpha$ -synuclein is ubiquitinated in  $\alpha$ -synucleinopathy lesions. *J. Biol. Chem.* **277**, 49071–49076
7. Tofaris, G. K., Razaq, A., Ghetti, B., Lilley, K. S., and Spillantini, M. G. (2003) Ubiquitination of  $\alpha$ -synuclein in Lewy bodies is a pathological event not associated with impairment of proteasome function. *J. Biol. Chem.* **278**, 44405–44411
8. Kuzuhara, S., Mori, H., Izumiya, N., Yoshimura, M., and Ihara, Y. (1988) Lewy bodies are ubiquitinated. A light and electron microscopic immunocytochemical study. *Acta Neuropathol.* **75**, 345–353
9. Tofaris, G. K., Kim, H. T., Horez, R., Jung, J. W., Kim, K. P., and Goldberg, A. L. (2011) Ubiquitin ligase Nedd4 promotes  $\alpha$ -synuclein degradation by the endosomal-lysosomal pathway. *Proc. Natl. Acad. Sci. U.S.A.* **108**, 17004–17009
10. Davies, S. E., Hallett, P. J., Moens, T., Smith, G., Mangano, E., Kim, H. T., Goldberg, A. L., Liu, J. L., Isacson, O., and Tofaris, G. K. (2014) Enhanced ubiquitin-dependent degradation by Nedd4 protects against  $\alpha$ -synuclein accumulation and toxicity in animal models of Parkinson's disease. *Neurobiol. Dis.* **64**, 79–87
11. Staub, O., Dho, S., Henry, P., Correa, J., Ishikawa, T., McGlade, J., and Rotin, D. (1996) WW domains of Nedd4 bind to the proline-rich PY motifs in the epithelial  $\text{Na}^+$  channel deleted in Liddle's syndrome. *EMBO J.* **15**, 2371–2380
12. Kanelis, V., Bruce, M. C., Skrynnikov, N. R., Rotin, D., and Forman-Kay, J. D. (2006) Structural determinants for high-affinity binding in a Nedd4 WW3\* domain-Comm PY motif complex. *Structure* **14**, 543–553
13. Wang, J., Peng, Q., Lin, Q., Childress, C., Carey, D., and Yang, W. (2010) Calcium activates Nedd4-E3 ubiquitin ligases by releasing the C2 domain-mediated auto-inhibition. *J. Biol. Chem.* **285**, 12279–12288
14. Dunn, R., and Hicke, L. (2001) Multiple roles for Rsp5p-dependent ubiquitination at the internalization step of endocytosis. *J. Biol. Chem.* **276**, 25974–25981
15. Hara, S., Arawaka, S., Sato, H., Machiya, Y., Cui, C., Sasaki, A., Koyama, S., and Kato, T. (2013) Serine 129 phosphorylation of membrane-associated  $\alpha$ -synuclein modulates dopamine transporter function in a G protein-coupled receptor kinase-dependent manner. *Mol. Biol. Cell* **24**, 1649–1660
16. Schröter, C. J., Braun, M., Englert, J., Beck, H., Schmid, H., and Kalbacher, H. (1999) A rapid method to separate endosomes from lysosomal contents using differential centrifugation and hypotonic lysis of lysosomes. *J. Immunol. Methods* **227**, 161–168
17. Rott, R., Szargel, R., Haskin, J., Shani, V., Shainskaya, A., Manov, I., Liani, E., Avraham, E., and Engelender, S. (2008) Monoubiquitylation of  $\alpha$ -sy-

## Nedd4-1 Targets Internalized $\alpha$ -Synuclein to Endosomes

- nuclein by seven in absentia homolog (SIAH) promotes its aggregation in dopaminergic cells. *J. Biol. Chem.* **283**, 3316–3328
18. Nagano, Y., Yamashita, H., Takahashi, T., Kishida, S., Nakamura, T., Iseki, E., Hattori, N., Mizuno, Y., Kikuchi, A., and Matsumoto, M. (2003) Siah-1 facilitates ubiquitination and degradation of synphilin-1. *J. Biol. Chem.* **278**, 51504–51514
  19. Shimura, H., Schlossmacher, M. G., Hattori, N., Frosch, M. P., Trockenbacher, A., Schneider, R., Mizuno, Y., Kosik, K. S., and Selkoe, D. J. (2001) Ubiquitination of a new form of  $\alpha$ -synuclein by parkin from human brain: implications for Parkinson's disease. *Science* **293**, 263–269
  20. Tetzlaff, J. E., Putcha, P., Outeiro, T. F., Ivanov, A., Berezovska, O., Hyman, B. T., and McLean, P. J. (2008) CHIP targets toxic  $\alpha$ -Synuclein oligomers for degradation. *J. Biol. Chem.* **283**, 17962–17968
  21. Anan, T., Nagata, Y., Koga, H., Honda, Y., Yabuki, N., Miyamoto, C., Kuwano, A., Matsuda, I., Endo, F., Saya, H., and Nakao, M. (1998) Human ubiquitin-protein ligase Nedd4: expression, subcellular localization and selective interaction with ubiquitin-conjugating enzymes. *Genes Cells* **3**, 751–763
  22. Nikko, E., and André, B. (2007) Evidence for a direct role of the Doa4 deubiquitinating enzyme in protein sorting into the MVB pathway. *Traffic* **8**, 566–581
  23. Lu, P. J., Zhou, X. Z., Shen, M., and Lu, K. P. (1999) Function of WW domains as phosphoserine- or phosphothreonine-binding modules. *Science* **283**, 1325–1328
  24. Georgieva, E. R., Ramlall, T. F., Borbat, P. P., Freed, J. H., and Eliezer, D. (2010) The lipid-binding domain of wild type and mutant  $\alpha$ -synuclein: compactness and interconversion between the broken and extended helix forms. *J. Biol. Chem.* **285**, 28261–28274
  25. Ahn, K. J., Paik, S. R., Chung, K. C., and Kim, J. (2006) Amino acid sequence motifs and mechanistic features of the membrane translocation of  $\alpha$ -synuclein. *J. Neurochem.* **97**, 265–279
  26. Varkey, J., Isas, J. M., Mizuno, N., Jensen, M. B., Bhatia, V. K., Jao, C. C., Petrova, J., Voss, J. C., Stamou, D. G., Steven, A. C., and Langen, R. (2010) Membrane curvature induction and tubulation are common features of  $\alpha$ -synucleins and apolipoproteins. *J. Biol. Chem.* **285**, 32486–32493
  27. Desplats, P., Lee, H. J., Bae, E. J., Patrick, C., Rockenstein, E., Crews, L., Spencer, B., Masliah, E., and Lee, S. J. (2009) Inclusion formation and neuronal cell death through neuron-to-neuron transmission of  $\alpha$ -synuclein. *Proc. Natl. Acad. Sci. U.S.A.* **106**, 13010–13015
  28. Tsigelny, I. F., Sharikov, Y., Wrasidlo, W., Gonzalez, T., Desplats, P. A., Crews, L., Spencer, B., and Masliah, E. (2012) Role of  $\alpha$ -synuclein penetration into the membrane in the mechanisms of oligomer pore formation. *FEBS J.* **279**, 1000–1013
  29. Lashuel, H. A., Overk, C. R., Oueslati, A., and Masliah, E. (2013) The many faces of  $\alpha$ -synuclein: from structure and toxicity to therapeutic target. *Nat. Rev. Neurosci.* **14**, 38–48
  30. Ren, P. H., Lauckner, J. E., Kachirskaja, I., Heuser, J. E., Melki, R., and Kopito, R. R. (2009) Cytoplasmic penetration and persistent infection of mammalian cells by polyglutamine aggregates. *Nat. Cell Biol.* **11**, 219–225
  31. Lin, A., Hou, Q., Jarzylo, L., Amato, S., Gilbert, J., Shang, F., and Man, H. Y. (2011) Nedd4-mediated AMPA receptor ubiquitination regulates receptor turnover and trafficking. *J. Neurochem.* **119**, 27–39
  32. Nabhan, J. F., Pan, H., and Lu, Q. (2010) Arrestin domain-containing protein 3 recruits the NEDD4 E3 ligase to mediate ubiquitination of the  $\beta$ 2-adrenergic receptor. *EMBO Rep.* **11**, 605–611
  33. Ingham, R. J., Gish, G., and Pawson, T. (2004) The Nedd4 family of E3 ubiquitin ligases: functional diversity within a common modular architecture. *Oncogene* **23**, 1972–1984
  34. Fujiwara, H., Hasegawa, M., Dohmae, N., Kawashima, A., Masliah, E., Goldberg, M. S., Shen, J., Takio, K., and Iwatsubo, T. (2002)  $\alpha$ -Synuclein is phosphorylated in synucleinopathy lesions. *Nat. Cell Biol.* **4**, 160–164
  35. Sugeno, N., Takeda, A., Hasegawa, T., Kobayashi, M., Kikuchi, A., Mori, F., Wakabayashi, K., and Itoyama, Y. (2008) Serine 129 phosphorylation of  $\alpha$ -synuclein induces unfolded protein response-mediated cell death. *J. Biol. Chem.* **283**, 23179–23188
  36. Rotin, D., and Kumar, S. (2009) Physiological functions of the HECT family of ubiquitin ligases. *Nat. Rev. Mol. Cell Biol.* **10**, 398–409
  37. Lauwers, E., Jacob, C., and André, B. (2009) Lys-63-linked ubiquitin chains as a specific signal for protein sorting into the multivesicular body pathway. *J. Cell Biol.* **185**, 493–502
  38. Galan, J. M., and Haguenaer-Tsapis, R. (1997) Ubiquitin lys63 is involved in ubiquitination of a yeast plasma membrane protein. *EMBO J.* **16**, 5847–5854
  39. Lauwers, E., Erpapazoglou, Z., Haguenaer-Tsapis, R., and André, B. (2010) The ubiquitin code of yeast permease trafficking. *Trends Cell Biol.* **20**, 196–204
  40. Tanikawa, S., Mori, F., Tanji, K., Kakita, A., Takahashi, H., and Wakabayashi, K. (2012) Endosomal sorting related protein CHMP2B is localized in Lewy bodies and glial cytoplasmic inclusions in  $\alpha$ -synucleinopathy. *Neurosci. Lett.* **527**, 16–21
  41. Kurashige, T., Takahashi, T., Yamazaki, Y., Hiji, M., Izumi, Y., Yamawaki, T., and Matsumoto, M. (2013) Localization of CHMP2B-immunoreactivity in the brainstem of Lewy body disease. *Neuropathology* **33**, 237–245
  42. Hayashida, K., Oyanagi, S., Mizutani, Y., and Yokochi, M. (1993) An early cytoplasmic change before Lewy body maturation: an ultrastructural study of the substantia nigra from an autopsy case of juvenile parkinsonism. *Acta Neuropathol.* **85**, 445–448
  43. Williams, R. L., and Urbé, S. (2007) The emerging shape of the ESCRT machinery. *Nat. Rev. Mol. Cell Biol.* **8**, 355–368
  44. Agromayor, M., and Martin-Serrano, J. (2006) Interaction of AMSH with ESCRT-III and deubiquitination of endosomal cargo. *J. Biol. Chem.* **281**, 23083–23091
  45. Cataldo, A. M., Peterhoff, C. M., Troncoso, J. C., Gomez-Isla, T., Hyman, B. T., and Nixon, R. A. (2000) Endocytic pathway abnormalities precede amyloid  $\beta$  deposition in sporadic Alzheimer's disease and Down syndrome: differential effects of APOE genotype and presenilin mutations. *Am. J. Pathol.* **157**, 277–286
  46. Nixon, R. A. (2004) Niemann-Pick type C disease and Alzheimer's disease: the APP-endosome connection fattens up. *Am. J. Pathol.* **164**, 757–761
  47. Gitler, A. D., Bevis, B. J., Shorter, J., Strathearn, K. E., Hamamichi, S., Su, L. J., Caldwell, K. A., Caldwell, G. A., Rochet, J. C., McCaffery, J. M., Barlowe, C., and Lindquist, S. (2008) The Parkinson's disease protein  $\alpha$ -synuclein disrupts cellular Rab homeostasis. *Proc. Natl. Acad. Sci. U.S.A.* **105**, 145–150
  48. Soper, J. H., Kehm, V., Burd, C. G., Bankaitis, V. A., and Lee, V. M. (2011) Aggregation of  $\alpha$ -synuclein in *S. cerevisiae* is associated with defects in endosomal trafficking and phospholipid biosynthesis. *J. Mol. Neurosci.* **43**, 391–405
  49. Tardiff, D. F., Jui, N. T., Khurana, V., Tambe, M. A., Thompson, M. L., Chung, C. Y., Kamadurai, H. B., Kim, H. T., Lancaster, A. K., Caldwell, K. A., Caldwell, G. A., Rochet, J. C., Buchwald, S. L., and Lindquist, S. (2013) Yeast reveal a "Druggable" Rsp5/Nedd4 network that ameliorates  $\alpha$ -synuclein toxicity in neurons. *Science* **342**, 979–983
  50. Freeman, D., Cedillos, R., Choyke, S., Lukic, Z., McGuire, K., Marvin, S., Burrage, A. M., Sudholt, S., Rana, A., O'Connor, C., Wiethoff, C. M., and Campbell, E. M. (2013)  $\alpha$ -Synuclein induces lysosomal rupture and cathepsin-dependent reactive oxygen species following endocytosis. *PLoS One* **8**, e62143